Precambrian Research 272 (2016) 203–225

Contents lists available at ScienceDirect

Precambrian Research

journal homepage: www.elsevier.com/locate/precamres

Early Neoproterozoic emplacement of the diabase sill swarms in the Liaodong Peninsula and pre-magmatic uplift of the southeastern North China Craton

Shuan-Hong Zhang[a,b,*], Yue Zhao[a,b], Hao Ye[a], Guo-Hui Hu[a]

[a] Institute of Geomechanics, Chinese Academy of Geological Sciences, Beijing 100081, China
[b] Key Laboratory of Paleomagnetism and Tectonic Reconstruction, Ministry of Land and Resources, Beijing 100081, China

ARTICLE INFO

Article history:
Received 2 September 2015
Received in revised form 4 November 2015
Accepted 12 November 2015
Available online 23 November 2015

Keywords:
Large igneous province (LIP)
Diabase sill (dyke) swarms
Continental rifting
Pre-magmatic (or pre-breakup) uplift
North China Craton (NCC)
Rodinia supercontinent

ABSTRACT

Diabase sill swarms are widespread within the Neoproterozoic sedimentary rocks in the Liaodong Peninsula (named as the Dalian mafic sill swarms), eastern North China Craton (NCC). Our new zircon LA-ICP-MS U–Pb and baddeleyite SIMS Pb–Pb dating results on five diabase sill samples emplaced into the Qiaotou, Cuijiatun and Xingmincun Formations in the Liaodong Peninsula indicate their emplacement during the early Neoproterozoic (Tonian) period at 0.92–0.89 Ga and pre-magmatic regional uplift prior to *ca.* 0.92–0.89 Ga. The above results provide important constraints on the upper boundary of the Neoproterozoic strata and their macroscopic carbonaceous fossils and organic-walled microfossils in the eastern and southeastern NCC and indicate they are Tonian in age. The early Neoproterozoic Dalian diabase sills belong to the tholeiitic series and are characterized by low contents of SiO_2 and K_2O, high contents of TiO_2, Fe_2O_3T and MgO, slight light REE (LREE)-enrichment and no Eu anomalies on chondrite-normalized REE patterns, enrichment of high field strength element (HFSE) and lack of negative Nb, Ta, Zr, Hf, P and Ti anomalies on primitive mantle-normalized spidergrams; and exhibit geochemical characteristics of within plate basalt on discrimination diagrams. The newly identified Dalian diabase sills, together with the previously reported Xu-Huai and Sariwon mafic sills and the Dashigou mafic dykes, constitute an early Neoproterozoic (0.92–0.89 Ga) large igneous province in the NCC (Sino-Korean Craton). Formation of the early Neoproterozoic diabase sill (dyke) swarms in the NCC is probably related to a continental rifting event that have led to breakup of southeastern NCC from some other continents in the Rodinia supercontinent. Breakup of the NCC from the Rodinia supercontinent at around 0.92–0.89 Ga is also supported by pre-magmatic regional uplift of the southeastern NCC prior to *ca.* 0.92–0.89 Ga and evolution trend of the Dalian diabase sills from within plate basalt to mid-ocean ridge basalt on the Zr/Y vs. Zr discrimination diagram.

1. Introduction

Mafic dyke (or sill) swarms are important indicators for widespread continental lithospheric extension and pointers of continental rifting and breakup events, and are very essential for ancient continental reconstructions (e.g., Halls, 1982; Fahrig, 1987; Kamo et al., 1989; Harris and Li, 1995; Ernst et al., 1995, 2008; Yale and Carpenter, 1998; Bleeker and Ernst, 2006; Hanski et al., 2006; Holm et al., 2006; Hou et al., 2008; Peng, 2010; Ernst, 2014). The North China Craton (NCC) is one of the oldest cratons in the world and experienced a complex geological evolution since the early Precambrian (Zhai and Santosh, 2013; Zhao and Zhai, 2013; Zhao, 2014 and references therein). Although most researchers believe that the NCC was involved in the assembly of the Columbia (also known as Nuna) supercontinent during the late Paleoproterozoic (e.g., Zhao et al., 2002, 2003, 2004, 2006, 2011; Wilde et al., 2002; Kusky et al., 2007; Kusky and Santosh, 2009; Santosh, 2010), whether or how the NCC was involved in the Meso-Neoproterozoic supercontinents (Columbia and Rodinia) and the position of the NCC in these supercontinents still remains unclear or controversial because of lack of reliable isotopic ages for Meso-Neoproterozoic (1.6–0.5 Ga) magmatism and tectonism in the NCC (e.g., Zhai, 2004; Lu et al., 2008). Thus, many paleogeographic reconstructions for the Columbia and Rodinia supercontinents during the Meso-Neoproterozoic time have excluded the NCC (e.g., Hoffman, 1991; Dalziel, 1991; Rogers

* Corresponding author at: No. 11 South Minzudaxue Road, Haidian District, Beijing 100081, China. Tel.: +86 10 88815058; fax: +86 10 68422326.
E-mail address: tozhangshuanhong@163.com (S.-H. Zhang).

http://dx.doi.org/10.1016/j.precamres.2015.11.005
0301-9268/

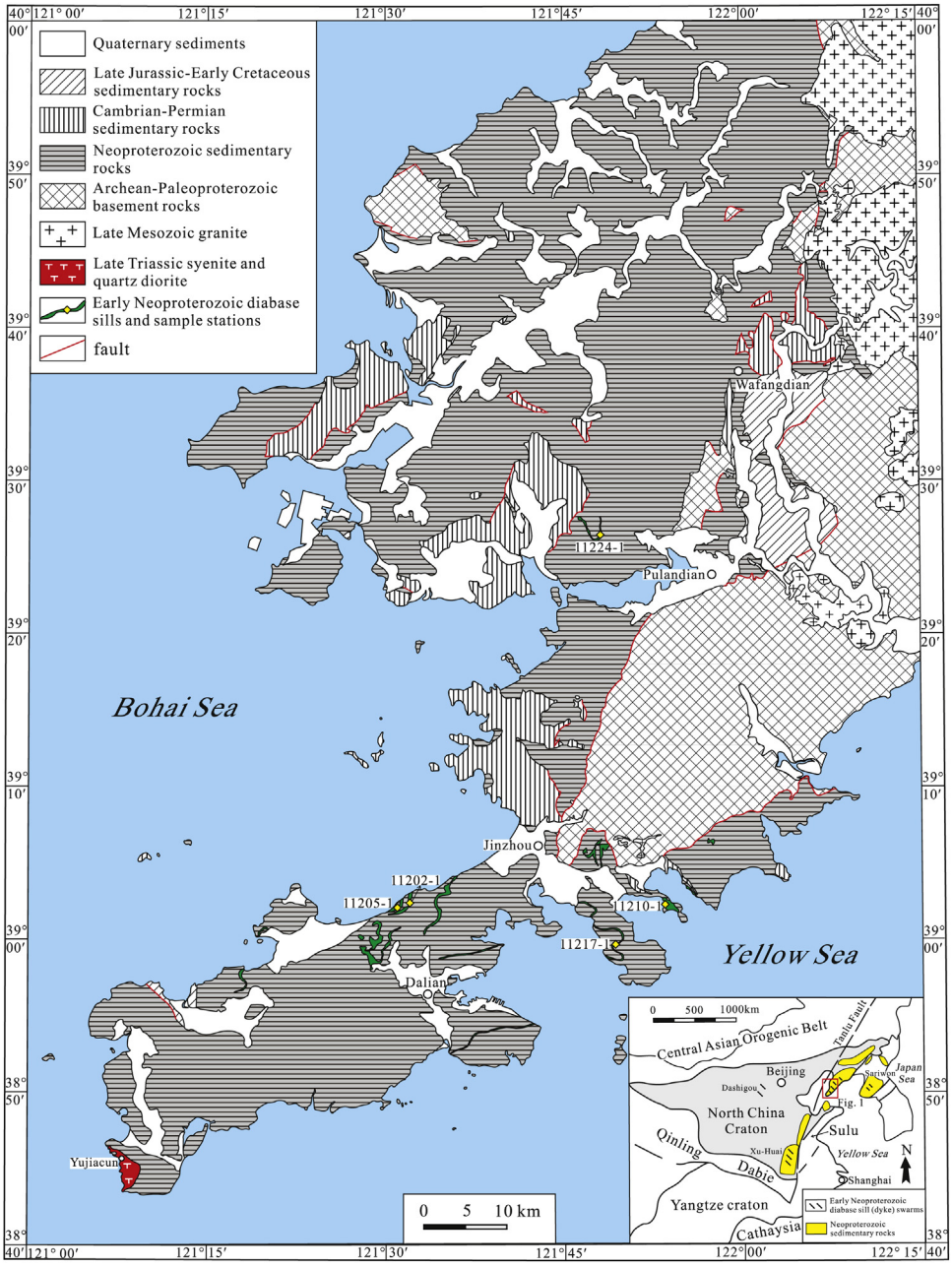

Fig. 1. Geological sketch map showing distribution of the diabase sills within the Neoproterozoic sedimentary rocks in the Liaodong Peninsula (modified after GSILP, 2001). Sample sites are also shown in the diagram.

and Santosh, 2002; Pesonen et al., 2003) or put it far away from other continents (e.g., Li et al., 2008). Recently, two stages of mafic sill (dyke) swarms, one in the Mid-Mesoproterozoic (1.35–1.32 Ga), another in the early Neoproterozoic (0.92–0.90 Ga), have been identified from the NCC (Liu et al., 2006; Gao et al., 2009; Zhang et al., 2009, 2012a; Li et al., 2009a; Peng et al., 2011a, 2011b; Wang et al., 2012; Peng, 2015). Moreover, several 1.23–1.21 Ga mafic intrusions have been identified from the eastern NCC (Peng et al., 2013; Wang et al., 2015). The Mid-Mesoproterozoic (1.35–1.32 Ga) mafic sill swarms were considered to be related to breakup of the northern NCC from the Columbia supercontinent (Zhang et al., 2009, 2012a; Wang et al., 2014a), which is supported by new paleomagnetic results (Zhang et al., 2012b; Chen et al., 2013; Xu et al., 2014). The early Neoproterozoic (0.92–0.90 Ga) mafic dyke (sill) swarms provide important evidence for involvement of the NCC in the Rodinia supercontinent. However, since sill (dyke) swarms associated with large igneous provinces do not always lead to breakup (e.g., Goldberg, 2010; Ernst, 2014), it is still uncertain whether they are related to local extension or breakup of the NCC from the Rodinia supercontinent because their ages are much older than the main period of the Rodinia breakup during the Mid-Neoproterozoic period (e.g., Karlstrom et al., 2001; Li et al., 2008; Evans, 2013).

In this contribution, we present new geological and geochronological evidence for early Neoproterozoic (Tonian) emplacement of the large volumes of diabase sills within the Neoproterozoic sedimentary rocks in the Liaodong Peninsula in the eastern NCC and regional uplift in the eastern NCC prior to *ca.* 0.92–0.89 Ga. The results presented in this study provide critical constraints on upper boundary of the Neoproterozoic strata and their macroscopic carbonaceous fossils and organic-walled microfossils in the eastern

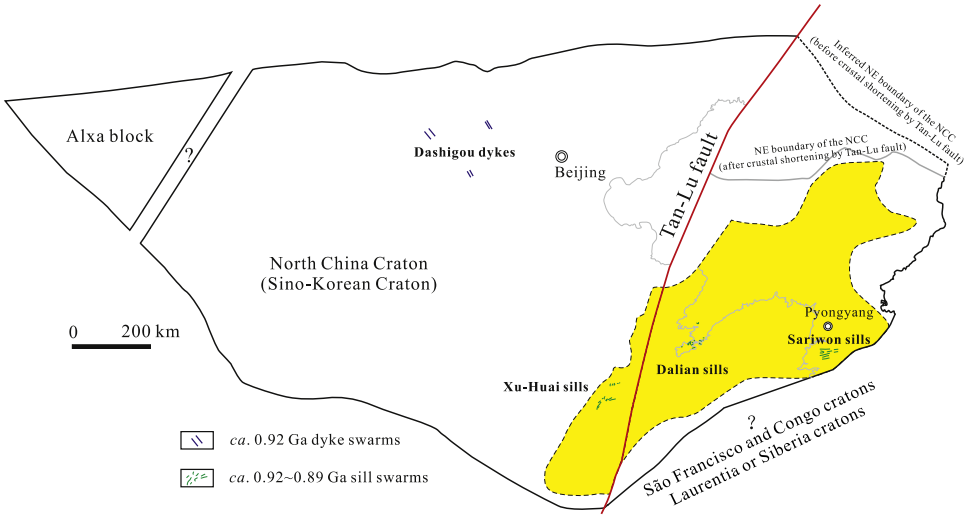

Fig. 2. A reconstruction map showing distribution of the early Neoproterozoic mafic sill (dyke) swarms in the NCC (Sino-Korean Craton) during the early Neoproterozoic period. The southeastern and northeastern boundaries of the NCC are reconstructed by considering the sinistral strike-slip motion of the Tan-Lu fault zone during the Triassic-Jurassic period and possibly crustal shortening in northeastern NCC induced by Tan-Lu fault. Yellow-shaded area shows distribution of the early Neoproterozoic sedimentary rocks in the southeastern NCC (For interpretation of the references to colour in this figure legend, the reader is referred to the web version of this article.).

and southeastern NCC as well as the timing and processes of continental rifting and breakup of the southeastern NCC from the Rodinia supercontinent.

2. Geological setting

The Liaodong Peninsula is located in the eastern NCC (Fig. 1). Prior to sinistral strike-slip motion of the Tan-Lu fault zone during the Triassic-Jurassic period (e.g., Xu et al., 1987; Zhu et al., 2005), it was located in the southeastern part of the NCC (Fig. 2). Its basement consists of highly metamorphosed Archean and Paleoproterozoic rocks, which are covered by a thick sequence of low-grade to unmetamorphosed Mesoproterozoic (Yushulazi Formation), Neoproterozoic (Yongning, Diaoyutai, Nanfen, Qiaotou, Changlingzi, Nanguanling, Ganjingzi, Yingchengzi, Shisanlitai, Majiatun, Cuijiatun and Xingmincun Formations, Fig. 3) and Cambrian-Ordovician marine clastic and carbonate platformal sediments, Middle Carboniferous to Early Permian shallow marine clastic rocks interbedding with terrigenous coal-bearing clastics, and Jurassic-Early Cretaceous terrestrial sediments and volcanic rocks (Fig. 1). Mesoproterozoic strata in the Liaodong Peninsula are about 3.5 km thick and the thickness of the Neoproterozoic strata is over 12.7 km (Fig. 3, GSILP, 2001). Since most of the previously regarded "Neoproterozoic" strata in northern and southern margins of the NCC were recently proved to be Mesoproterozoic in age by high-precision SHRIMP or LA-ICP-MS U–Pb dating (e.g., Gao et al., 2007, 2008; Zhang et al., 2009, 2012a; Lu et al., 2010; Su et al., 2012), the Liaodong Peninsula became one of the few remaining places with exposure of complete sequences of the Neoproterozoic strata in the NCC.

Similar to other parts of the NCC, there is no angular unconformity between strata from the Mesoproterozoic to Early Permian. From Middle Triassic, the Liaodong Peninsula was strongly deformed with emplacement of large volumes of Mesozoic granitoid intrusions (e.g., Xu et al., 1991; Yang et al., 1996, 2002, 2007a, 2011; Bing and Wang, 2004; Wu et al., 2005; Liu et al., 2005b; Lin et al., 2011). Middle-Late Triassic deformation, which is probably related to overriding plate deformation of the Sulu continent–continent collision, is strongly affected by near N–S contraction with development of large scale folding in the Meso-Neoproterozoic to Early Permian strata (Yang et al., 2002, 2011; Bing and Wang, 2004). In the Early Cretaceous, the Liaodong Peninsula is characterized by NW–SE extension with development of extensional volcano-sedimentary basins and metamorphic core complexes (e.g., Yang et al., 1996; Liu et al., 2005b; Lin et al., 2011).

3. Field occurrence and sample description

Diabase intrusions are very common in the Liaodong Peninsula and occur mainly as sills within the Neoproterozoic Yongning, Qiaotou, Changlingzi, Nanguanling, Ganjingzi, Yingchengzi, Cuijiatun and Xingmincun Formations. The diabase sills are usually several meters to several hundred meters thick and several hundred meters to over ten kilometers long (Fig. 1). At least three layers of diabase sills exist within the Ganjingzi Formation near Dalashufang along the western coast of the Liaodong Peninsula (Fig. 4A). Near the boundary of sills, baked zones are very common in sandstones and siltstones and the dolomites and limestones display recrystallization due to thermal emplacement of diabase sills (Fig. 5D, E). Usually these diabase sills were folded with the surrounding strata, indicating their emplacement prior to regional folding during the Middle-Late Triassic. They exhibit coarse-, medium- to fine-grained ophitic texture with similar mineral compositions of clinopyroxene (45–65 vol.%), plagioclase (30–55 vol.%), hornblende (0–5 vol.%) and Fe–Ti oxides (magnetite and ilmenite, 0–5 vol.%) and minor quartz, K-feldspar and biotite (Fig. 6). Some diabase sills are characterized by exfoliate concentric weathering near surface (Fig. 5). Similar to the Meso-Neoproterozoic sedimentary rocks in the Liaodong Peninsula, the diabase sills underwent no intense metamorphism. Most plagioclase has experienced saussuritization and some clinopyroxene was altered to chlorite, biotite and uralite.

Over twenty large diabase samples (>15 kg) emplaced into the Neoproterozoic sedimentary rocks in different places in the Liaodong Peninsula were collected to separate zircons and baddeleyites for U–Pb/Pb–Pb geochronology. Among them four samples yield sufficient zircon grains and three samples yield sufficient baddeleyite grains for dating. Description of the geochronological samples is listed below.

Sample 11224-1 is a medium-grained diabase collected from a sill emplaced into the Qiaotou Formation northwest to Pulandian (GPS position: E121°48.05′; N39°26.22′). It is composed of clinopyroxene (58 vol.%), plagioclase (39 vol.%) and Fe–Ti oxides (magnetite and ilmenite, 3 vol.%), with accessory apatite, zircon and titanite. Zircons from this sample are transparent-semitransparent,

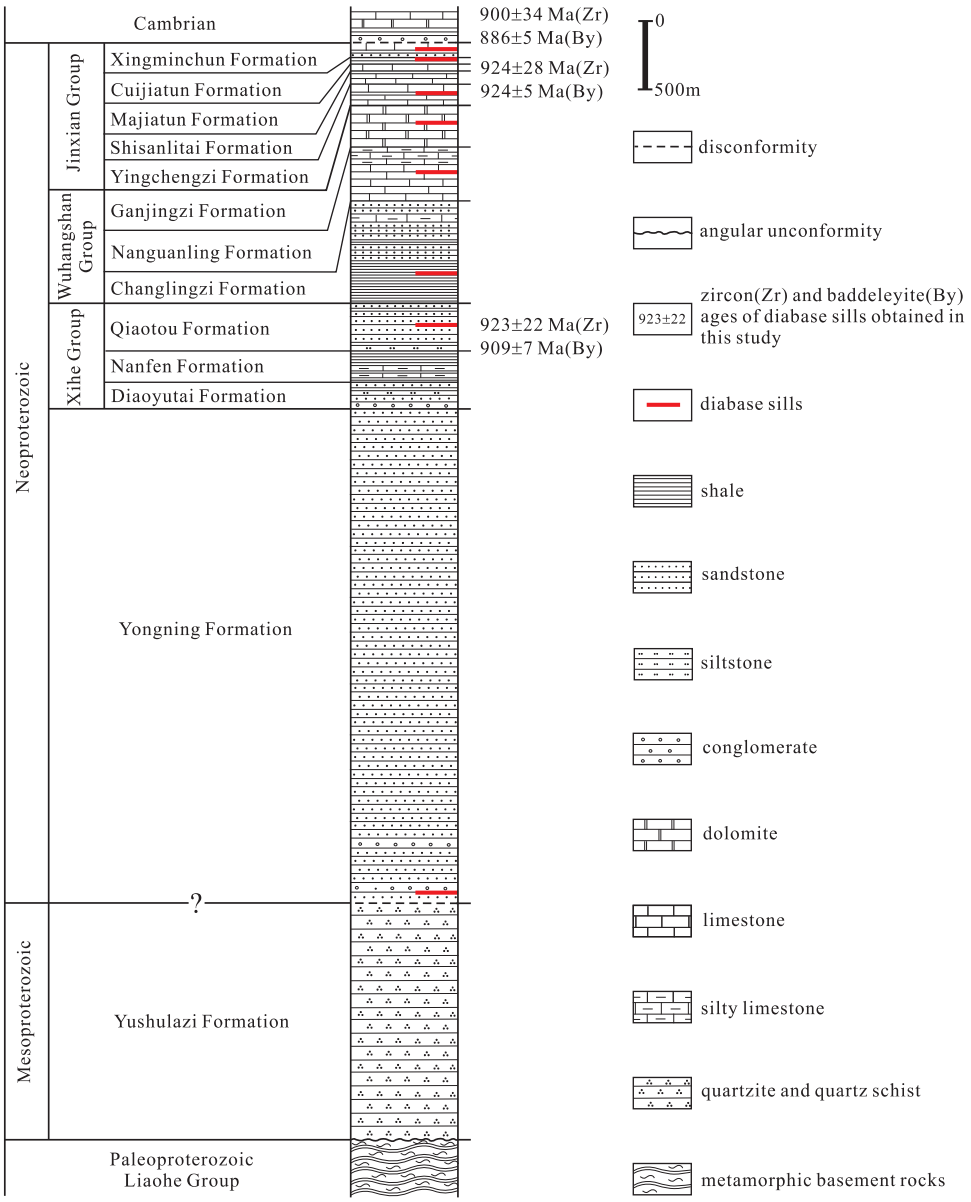

Fig. 3. Stratigraphic column of the Meso-Neoproterozoic sedimentary rocks in the Liaodong Peninsula (modified after GSILP, 2001).

creamy white-pink, euhedral or subhedral prisms with a size ranging from 50 to 180 μm and length/width ratio of 1:1 to 2:1. They are quite homogeneous and exhibit weak oscillatory zoning in cathodoluminescence (CL) images (Fig. 7A). Some zircons are characterized by thin schlieren parallel to their long axis.

Sample 11210-1 is a coarse-grained diabase collected from a sill emplaced into the Xingmincun Formation near Wangjiatun along the eastern coast of the Liaodong Peninsula (GPS position: E121°53.27′; N39°02.59′). It consists of plagioclase (35 vol.%), clinopyroxene (60 vol.%) and Fe–Ti oxides (magnetite and ilmenite, 5 vol.%), with accessory apatite, zircon, baddeleyite and titanite. Zircons from this sample are transparent-semitransparent, pink euhedral prisms with a size ranging from 30 to 150 μm and length/width ratio of 1:1–3.5:1. In CL images, they are quite homogeneous and exhibit weak oscillatory zoning (Fig. 7B). Some zircons exhibit thin schlieren parallel to their long axis. Baddeleyites are brown euhedral small platy prisms with a size ranging from 30 to 60 μm. They exhibit homogeneous structures in CL and backscattered electron (BSE) images (Fig. 8B).

Sample 11205-1 is a weathered medium-grained diabase collected from a sill emplaced into the Cuijiatun and Xingmincun Formations north to Gezhenbu along the western coast of the Liaodong Peninsula (GPS position: E121°31.11′; N39°01.75′). Its mineral assemblage is clinopyroxene (50 vol.%), plagioclase (48 vol.%) and Fe–Ti oxides (magnetite and ilmenite, 2 vol.%), with accessory apatite, zircon and baddeleyite. The zircons are transparent-semitransparent-opaque, creamy white-pink, and euhedral prisms with length/width ratio of 1:1 to 3:1. The grain sizes are from 50 to 100 μm. They are very homogeneous and exhibit weak or no oscillatory zoning in CL images (Fig. 7C). Most zircons from this sample are characterized by thin schlieren parallel to their long axis. Baddeleyites are brown euhedral platy prisms with a size ranging from 30 to 150 μm. They are quite homogeneous in CL and BSE images (Fig. 8A).

Sample 11202-1 is another weathered medium-grained diabase collected from a sill emplaced into the Cuijiatun and Xingmincun Formations north to Gezhenbu along the western coast of the Liaodong Peninsula (GPS position: E121°32.02′; N39°02.41′).

Table 1
LA-ICP-MS U–Pb dating results of zircons from the diabase sill swarms in the Liaodong Peninsula.

Grain-spot	Total Pb (ppm)	^{232}Th (ppm)	^{238}U (ppm)	^{232}Th/^{238}U	Isotopic ratios					
					^{207}Pb/^{206}Pb	±1σ	^{207}Pb/^{235}U	±1σ	^{206}Pb/^{238}U	±1σ
Sample 11224-1 (Liaodong Peninsula, diabase sills emplaced into the Qiaotou Formation; GPS position: E121°48.05′; N39°26.22′)										
01	853	994	632	1.57	0.0701	0.0013	1.6221	0.0323	0.1663	0.0017
02	709	1106	850	1.30	0.0680	0.0013	1.1303	0.0215	0.1193	0.0010
03	781	897	691	1.30	0.0705	0.0013	1.5666	0.0286	0.1596	0.0012
04	755	1341	939	1.43	0.0675	0.0013	1.0281	0.0245	0.1092	0.0016
05	624	748	664	1.13	0.0704	0.0014	1.4926	0.0320	0.1524	0.0015
06	894	1027	737	1.39	0.0739	0.0016	1.6413	0.0346	0.1599	0.0014
07	564	631	552	1.14	0.0703	0.0015	1.5752	0.0343	0.1615	0.0013
08	583	644	554	1.16	0.0710	0.0015	1.6024	0.0331	0.1625	0.0013
09	600	756	612	1.23	0.0700	0.0013	1.4522	0.0293	0.1494	0.0014
10	272	287	289	0.99	0.0723	0.0021	1.6689	0.0486	0.1662	0.0018
11	832	1017	751	1.35	0.0699	0.0015	1.4788	0.0316	0.1519	0.0011
12	1240	1895	1100	1.72	0.0692	0.0015	1.2128	0.0269	0.1260	0.0012
13	520	581	508	1.14	0.0701	0.0016	1.5959	0.0372	0.1637	0.0014
14	637	697	600	1.16	0.0703	0.0015	1.6965	0.0415	0.1731	0.0023
15	782	906	654	1.38	0.0699	0.0015	1.6167	0.0435	0.1649	0.0024
16	587	664	577	1.15	0.0679	0.0015	1.5759	0.0347	0.1658	0.0015
17	616	688	575	1.20	0.0680	0.0015	1.5143	0.0315	0.1591	0.0013
18	674	796	563	1.41	0.0688	0.0017	1.5386	0.0373	0.1594	0.0017
Sample 11210-1 (Liaodong Peninsula, diabase sills emplaced into the Xingmincun Formation; GPS position: E121°53.27′; N39°02.59′)										
01	323	369	289	1.27	0.0754	0.0027	1.9156	0.0740	0.1828	0.0038
02	2072	10300	3794	2.71	0.0624	0.0012	0.4544	0.0100	0.0520	0.0006
03	1723	9530	3327	2.86	0.0593	0.0012	0.3867	0.0076	0.0469	0.0005
04	655	1239	796	1.56	0.0685	0.0015	1.2220	0.0260	0.1282	0.0011
05	911	2885	1665	1.73	0.0648	0.0014	0.7033	0.0165	0.0778	0.0007
06	534	844	640	1.32	0.0680	0.0016	1.3689	0.0321	0.1449	0.0012
07	831	1236	823	1.50	0.0683	0.0017	1.4909	0.0376	0.1566	0.0014
08	994	3053	1807	1.69	0.0602	0.0014	0.6248	0.0164	0.0744	0.0010
09	792	1240	708	1.75	0.0708	0.0017	1.5622	0.0407	0.1587	0.0024
10	2788	10631	3515	3.02	0.0648	0.0015	0.6430	0.0170	0.0710	0.0010
11	374	638	492	1.30	0.0686	0.0021	1.3684	0.0404	0.1433	0.0018
12	806	3369	2195	1.54	0.0634	0.0016	0.5267	0.0131	0.0594	0.0006
13	545	855	650	1.32	0.0735	0.0023	1.4698	0.0452	0.1433	0.0018
14	1080	2713	1263	2.15	0.0653	0.0015	0.9347	0.0236	0.1023	0.0014
15	1328	2472	1294	1.91	0.0672	0.0013	1.2390	0.0246	0.1319	0.0011
16	973	1574	899	1.75	0.0684	0.0015	1.4257	0.0313	0.1493	0.0013
17	880	3028	1619	1.87	0.0681	0.0013	0.7069	0.0146	0.0744	0.0008
18	802	1478	769	1.92	0.0691	0.0018	1.3536	0.0426	0.1403	0.0027
Sample 11205-1 (Liaodong Peninsula, diabase sills emplaced into the Cuijiatun and Xingmincun Formations; GPS position: E121°31.11′; N39°01.75′)										
01	835	1134	1040	1.09	0.0701	0.0013	1.3195	0.0240	0.1351	0.0011
02	527	631	648	0.97	0.0704	0.0014	1.5253	0.0306	0.1556	0.0014
03	1231	2492	1590	1.57	0.0648	0.0013	0.8811	0.0210	0.0974	0.0013
04	848	1085	814	1.33	0.0693	0.0014	1.4771	0.0302	0.1531	0.0012
05	781	2066	1865	1.11	0.0653	0.0015	0.6303	0.0151	0.0693	0.0008
06	1126	3118	1852	1.68	0.0655	0.0016	0.6514	0.0174	0.0714	0.0010
07	1301	2139	1416	1.51	0.0683	0.0015	1.1281	0.0260	0.1185	0.0013
08	1009	1366	1142	1.20	0.0719	0.0014	1.3695	0.0297	0.1366	0.0013
09	323	141	212	0.67	0.1577	0.0029	9.0622	0.2021	0.4118	0.0056
10	570	654	476	1.37	0.0794	0.0017	1.7499	0.0366	0.1581	0.0012
11	636	733	743	0.99	0.0700	0.0014	1.5538	0.0316	0.1599	0.0020
12	1078	1837	1253	1.47	0.0681	0.0014	1.0852	0.0225	0.1142	0.0009
13	1237	2629	1571	1.67	0.0666	0.0014	0.8411	0.0208	0.0904	0.0013
14	725	836	654	1.28	0.0847	0.0020	1.8479	0.0473	0.1555	0.0014
15	891	3089	2697	1.15	0.0653	0.0012	0.5086	0.0117	0.0563	0.0010
16	1249	3004	1911	1.57	0.0631	0.0012	0.6971	0.0186	0.0792	0.0016
17	1521	6780	3937	1.72	0.0653	0.0014	0.3898	0.0097	0.0427	0.0005
18	992	1720	1165	1.48	0.0703	0.0015	1.1915	0.0364	0.1204	0.0025
Sample 11202-1 (Liaodong Peninsula, diabase sills emplaced into the Cuijiatun and Xingmincun Formations; GPS position: E121°32.02′; N39°02.41′)										
01	341	389	358	1.09	0.0695	0.0022	1.5622	0.0499	0.1599	0.0019
02	1431	5552	3258	1.70	0.0662	0.0015	0.4551	0.0105	0.0490	0.0006
03	1351	4136	1814	2.28	0.0676	0.0016	0.6013	0.0173	0.0633	0.0012
04	1354	4683	2970	1.58	0.0634	0.0012	0.4823	0.0110	0.0544	0.0009
05	954	2676	2295	1.17	0.0680	0.0011	0.7093	0.0259	0.0746	0.0026
06	2066	5114	1302	3.93	0.0666	0.0015	0.8004	0.0211	0.0858	0.0010

Table 1 (*Continued*)

Grain-spot	Isotopic ages (Ma)					
	$^{207}Pb/^{206}Pb$	±1σ	$^{207}Pb/^{235}U$	±1σ	$^{206}Pb/^{238}U$	±1σ
Sample 11224-1 (Liaodong Peninsula, diabase sills emplaced into the Qiaotou Formation; GPS position: E121°48.05′; N39°26.22′)						
01	931	24	979	13	992	10
02	878	25	768	10	727	6
03	943	25	957	11	955	7
04	854	26	718	12	668	9
05	939	28	927	13	915	9
06	1039	29	986	13	956	8
07	936	31	960	14	965	7
08	959	29	971	13	971	7
09	928	26	911	12	897	8
10	994	41	997	18	991	10
11	928	31	922	13	912	6
12	906	30	806	12	765	7
13	931	34	969	15	977	8
14	937	29	1007	16	1029	13
15	928	32	977	17	984	13
16	865	31	961	14	989	8
17	878	29	936	13	952	7
18	894	33	946	15	954	9
Sample 11210-1 (Liaodong Peninsula, diabase sills emplaced into the Xingmincun Formation; GPS position: E121°53.27′; N39°02.59′)						
01	1080	45	1087	26	1082	21
02	687	28	380	7	327	4
03	576	26	332	6	295	3
04	885	30	811	12	778	6
05	769	34	541	10	483	4
06	878	34	876	14	872	7
07	880	37	927	15	938	8
08	609	33	493	10	463	6
09	952	30	955	16	950	13
10	769	33	504	11	442	6
11	887	40	875	17	863	10
12	724	35	430	9	372	4
13	1028	42	918	19	863	10
14	785	31	670	12	628	8
15	843	27	818	11	799	6
16	880	30	900	13	897	8
17	870	25	543	9	463	5
18	902	35	869	18	846	15
Sample 11205-1 (Liaodong Peninsula, diabase sills emplaced into the Cuijiatun and Xingmincun Formations; GPS position: E121°31.11′; N39°01.75′)						
01	931	24	854	11	817	6
02	939	27	941	12	932	8
03	769	29	642	11	599	8
04	906	29	921	12	919	7
05	787	31	496	9	432	5
06	791	32	509	11	445	6
07	880	30	767	12	722	7
08	983	29	876	13	825	7
09	2431	20	2344	20	2223	25
10	1183	29	1027	14	946	7
11	931	23	952	13	956	11
12	872	30	746	11	697	5
13	833	29	620	11	558	7
14	1309	36	1063	17	932	8
15	787	22	417	8	353	6
16	722	27	537	11	491	9
17	783	31	334	7	270	3
18	939	31	797	17	733	15
Sample 11202-1 (Liaodong Peninsula, diabase sills emplaced into the Cuijiatun and Xingmincun Formations; GPS position: E121°32.02′; N39°02.41′)						
01	922	46	955	20	956	11
02	813	29	381	7	308	4
03	857	31	478	11	396	7
04	720	24	400	8	341	5
05	869	34	544	15	464	15
06	833	35	597	12	531	6

It is composed of clinopyroxene (47 vol.%), plagioclase (50 vol.%) and Fe–Ti oxides (magnetite and ilmenite, 3 vol.%), with accessory apatite and zircon. Zircons from this sample are semitransparent-opaque, creamy white-pink, euhedral or subhedral prisms with a size ranging from 50 to 200 μm and length/width ratio of 1:1 to 3:1. In CL images, they are very homogeneous and exhibit weak or no oscillatory zoning (Fig. 7D). Some zircons exhibit thin schlieren parallel to their long axis.

Sample 11217-1 is a coarse-grained diabase collected from a sill emplaced into the Qiaotou Formation near Dagushan along the

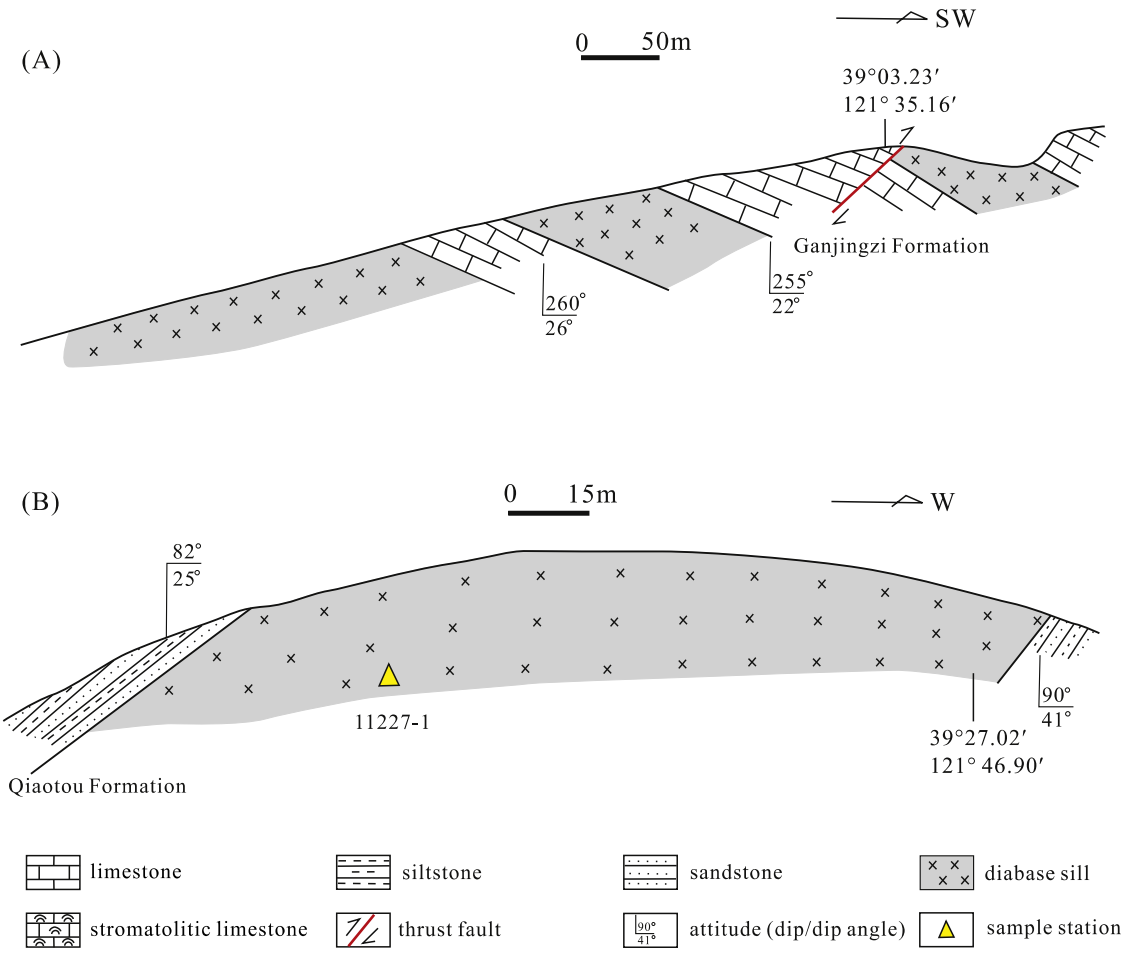

Fig. 4. Geological sections showing the diabase sills within the Neoproterozoic sedimentary rocks in the Liaodong Peninsula. (A) Diabase sills emplaced into the Ganjingzi Formation near Dalashufang along the western coast of the Liaodong Peninsula; (B) diabase sill emplaced into the Qiaotou Formation northwest to Pulandian.

eastern coast of the Liaodong Peninsula (GSP position: E121°49.68′; N38°59.71′). It consists of plagioclase (33 vol.%), clinopyroxene (60 vol.%), hornblende (2 vol.%) and Fe–Ti oxides (magnetite and ilmenite, 5 vol.%), with accessory apatite and baddeleyite. Its baddeleyite are brown euhedral platy prisms with a size ranging from 30 to 150 μm and exhibiting homogeneous structures in CL and BSE images (Fig. 8C).

4. Methods and analytical procedures

4.1. Sample preparation and imaging

Zircons and baddeleyites were separated using conventional crushing and separation techniques and were then handpicked under a binocular microscope. They were mounted in epoxy resin and polished to expose the cores of the grains in readiness for photomicrograph, CL, BSE, and LA-ICP-MS U–Pb or SIMS Pb–Pb analyses. Zircons and baddeleyites were imaged using the LEO 1450VP scanning electron microscope attached with GATAN Mini-CL detector at the Institute of Geology and Geophysics, Chinese Academy of Sciences, Beijing. CL images of the analyzed zircon grains are shown in Fig. 7. CL and BSE images of the analyzed baddeleyite grains are shown in Fig. 8.

4.2. Zircon LA-ICP-MS U–Pb and trace element analysis

U–Pb dating and trace element analyses of zircon were conducted synchronously by LA-ICP-MS at the State Key Laboratory of Geological Processes and Mineral Resources, China University of Geosciences, Wuhan. Detailed operating conditions for the laser ablation system and the ICP-MS instrument and data reduction are the same as description in Liu et al. (2008, 2010a, 2010b). The ICP-MS used is an Agilent 7500a. The GeoLas 2005 laser-ablation system was used for the laser ablation experiments. Nitrogen was added into the central gas flow (Ar + He) of the Ar plasma to decrease the detection limit and improve precision (Hu et al., 2008). Sites for analyses were selected on the basis of CL and photomicrograph images. The spots used were 30–32 μm in diameter. U, Th and Pb concentrations were calibrated by using ^{29}Si as an internal standard and NIST SRM 610 as the reference standard. Isotopic ratios were calculated using ICPMSDataCal 7.7 (Liu et al., 2008, 2010a), which were then corrected for both instrumental mass bias and depth-dependent elemental and isotopic fractionation using Harvard zircon 91500 (Wiedenbeck et al., 1995) as an external standard. Concordia diagrams and weighted mean ages were produced using the program ISOPLOT/Ex 3.23 (Ludwig, 2003).

4.3. Baddeleyite SIMS Pb–Pb dating

Baddeleyite SIMS Pb–Pb dating was performed on a Cameca IMS 1280-HR large-radius ion microprobe at the Institute of Geology and Geophysics, Chinese Academy of Sciences, Beijing following the method of Li et al. (2009b, 2010). The ellipsoidal spot is about 20 μm × 30 μm in size. The multi-collector mode equipped with four ion counting EMs was used to measure secondary ion beam intensities of ^{204}Pb, ^{206}Pb, ^{207}Pb and ^{208}Pb at a mass resolution of

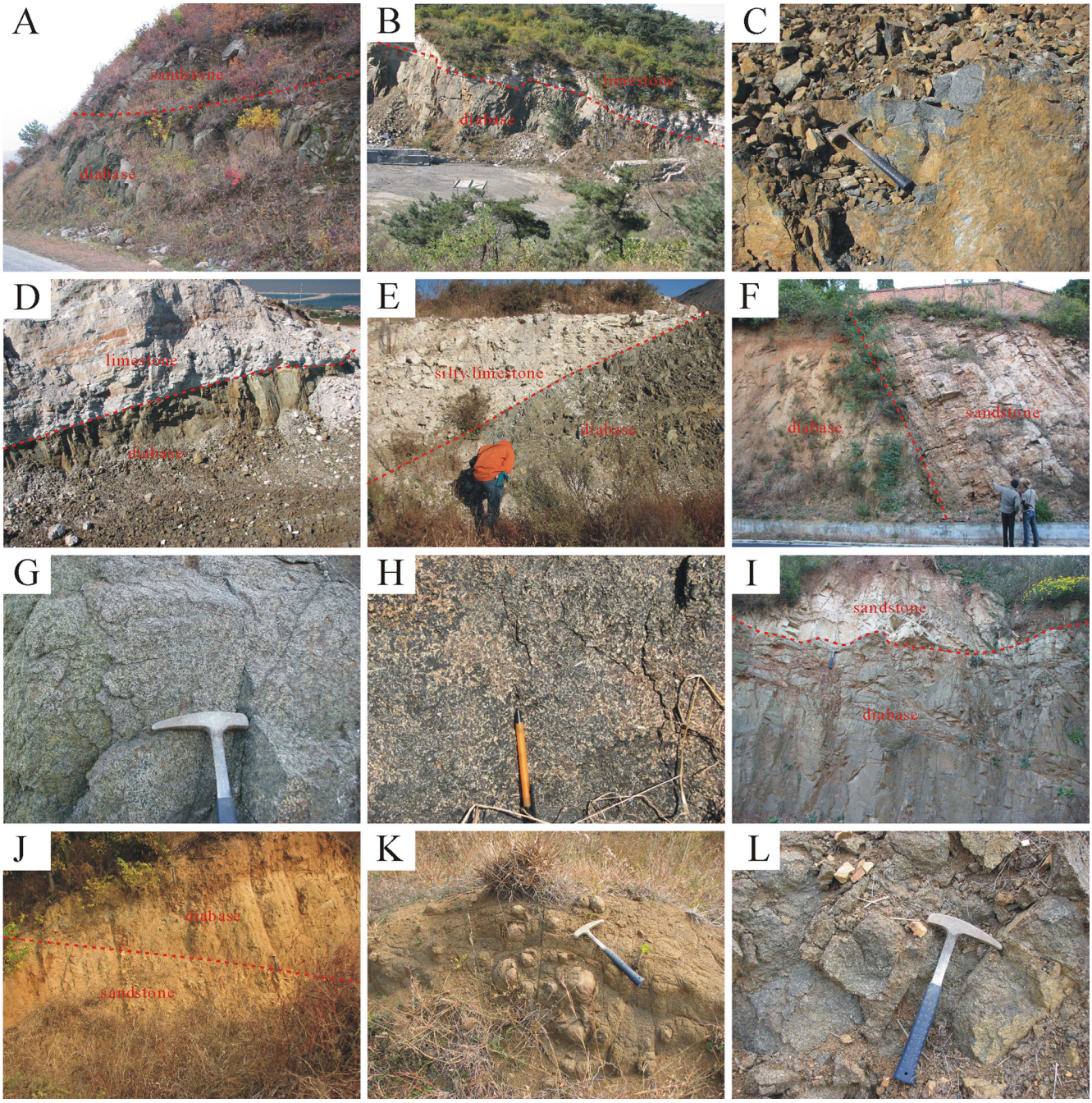

Fig. 5. Field photograph of typical diabase sills emplaced into the Neoproterozoic sedimentary rocks in the Liaodong Peninsula. (A) Diabase sill emplaced into the sandstone of the Yongning Formation (E122°52.31′; N40°09.28′); (B) diabase sill emplaced into the limestone (recrystallized to white marble) of the Ganjingzi Formation (E121°35.16′; N39°03.23′); (C) medium-grained diabase within the Ganjingzi Formation (E121°35.33′; N39°03.37′); (D) diabase sill emplaced into the limestone (recrystallized to white marble) of the Ganjingzi Formation (E121°35.35′; N39°03.40′); (E) diabase sill emplaced into the silty limestone (recrystallized to white marble) of the Ganjingzi Formation (E121°34.62′; N39°01.91′); (F) diabase sill emplaced into the sandstone of the Qiaotou Formation (E121°49.68′; N38°59.71′); (G) medium-grained diabase within the Xingmincun Formation (E121°53.27′; N39°02.59′); (H) coarse-grained diabase within the Xingmincun Formation (E121°53.27′; N39°02.59′); (I) diabase sill emplaced into the sandstone of the Cuijiatun Formation (E121°53.37′; N39°01.98′); (J) diabase sill emplaced into the sandstone of the Qiaotou Formation (E121°47.75′; N39°26.11′); (K) spheriodal weathering of diabase within the Qiaotou Formation (E121°48.05′; N39°26.22′); (L) coarse- to medium-grained diabase within the Qiaotou Formation (E121°47.00′; N39°27.00′).

~8000 (at 50% peak height, fixed exit slit). The ^{206}Pb signal was used as reference peak for tuning the secondary ions. The standard Phalaborwa was used to calibrate the Pb/U ratio and U concentration (Heaman and LeCheminant, 1993; Heaman, 2009). For Pb isotopes analyses, each measurement consists of 70 cycles, and the total analytical time is ca. 12 min. The radiogenic $^{207}Pb/^{206}Pb$ ratios of baddeleyite were calculated by correction of common Pb using non-radiogenic ^{204}Pb. Weighted mean ages were calculated using the program ISOPLOT/Ex 3.23 (Ludwig, 2003).

4.4. Major and trace element geochemistry

Major elements except FeO were analyzed on fused glass discs by X-ray fluorescence spectrometry and FeO contents by

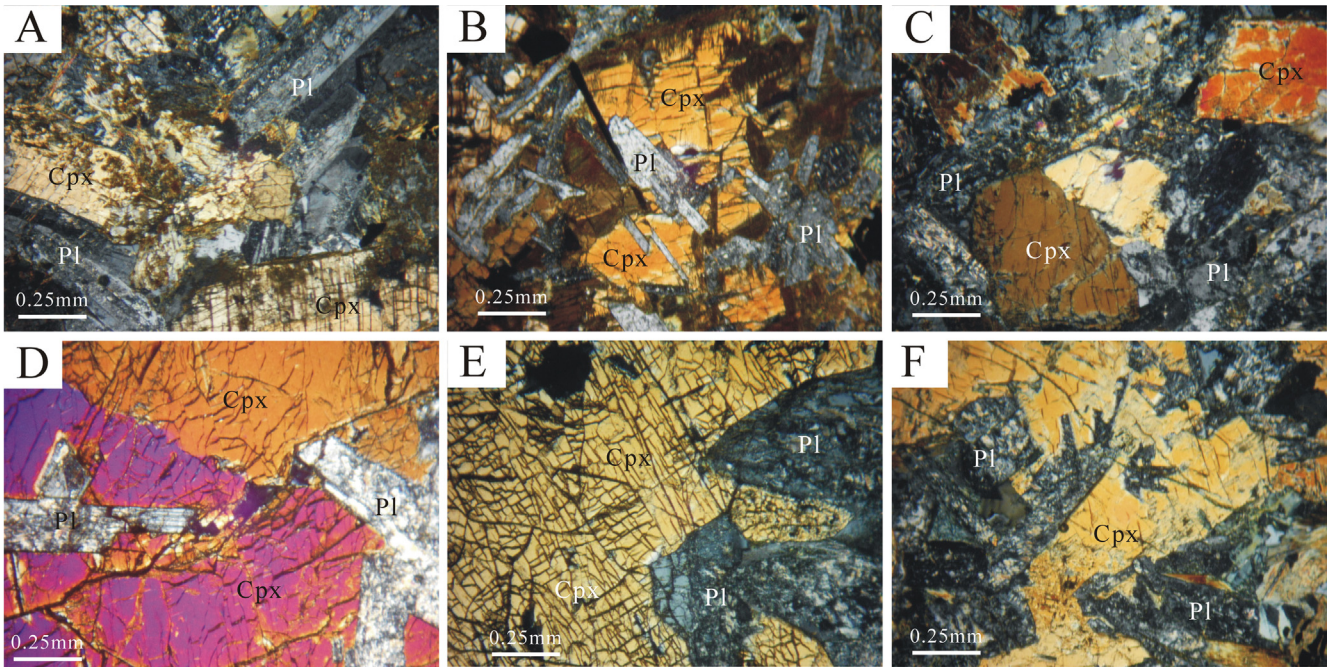

Fig. 6. Photomicrograph (cross-polarized light) of typical diabase samples within the Neoproterozoic sedimentary rocks in the Liaodong Peninsula. (A) Medium-grained diabase within the Ganjingzi Formation (sample 11199-1); (B) medium-grained diabase within the Cuijiatun and Xingmincun Formations (sample 11203-1); (C) medium-grained diabase within the Changlingzi Formation (sample 11207-1); (D), (E) coarse-grained diabase within the Xingmincun Formation (sample 11210-1); (F) coarse- to medium-grained diabase within the Qiaotou Formation (sample 11224-1). Mineral abbreviations: Cpx, clinopyroxene; Pl, plagioclase.

classical wet chemical analysis at the Analytical Laboratory of the Beijing Research Institute of Uranium Geology. Trace elements (including REE) were determined by ICP-MS (Agilent 7700e ICP-MS) at the Wuhan Sample Solution Analytical Technology Company Limited, Wuhan, China. About 50 mg whole-rock powders were weighed and then dissolved in distilled HF-HNO_3 in Teflon screw-cap beakers and high-pressure Teflon bombs at 190 °C for over 24 h, dried and then digested with HNO_3 at 140 °C for 1 day. The sample was re-dissolved by adding 1 ml HNO_3, 1 ml MQ H_2O and 1 ml internal standard In, and resealed and heated in the bomb at 190 °C for over 12 h. The final solution was diluted to 100 g with mixture of 2% HNO_3 for ICP-MS analysis. Indium was used as an internal standard to correct for matrix effects and instrument drift. Four international standards AGV-2 (andesite), BHVO-2 (basalt), BCR-2 (basalt) and RGM-2 (rhyolite) were used to monitor analyses. Errors for major element analysis are within 1%, except for P_2O_5 (5%), and analyses for most trace elements (including REE) are within 10%.

5. Results

5.1. Zircon U–Pb geochronology

Zircons from four diabase samples were analyzed using the LA-ICP-MS method. The analytical results are listed in Table 1 and plotted on concordia diagrams in Fig. 9. Usually, zircons with high contents of U (>1200 ppm) usually have suffered substantial Pb loss; however, those with low contents of U (<1100 ppm) usually yield concordant ages with concordance >95%.

Eighteen spots on 18 zircon grains from sample 11224-1 emplaced into the Qiaotou Formations were dated and most of the analyses are concordant. Although three analyses (spots 02, 04 and 12) are not concordant due to minor amounts of Pb loss (Fig. 9A), their $^{207}Pb/^{206}Pb$ ages are well concentrated. The weighted mean $^{207}Pb/^{206}Pb$ age of all analyses is 923 ± 22 Ma (95% confidence, MSWD = 2.3, N = 18). Different to the synmagmatic zircons from intermediate-acid igneous rock that are characterized by oscillatory zoning, zircons from the diabase sample are quite homogeneous and exhibit weak oscillatory zoning in CL images (Fig. 7A) and show high Th/U ratios (0.99–7.70, Table 1), indicating they are magmatic in origin. The above characteristics are very similar to those of the synmagmatic zircons from the diabase samples in the NCC (e.g., Liu et al., 2006; Gao et al., 2009; Zhang et al., 2009, 2012a; Wang et al., 2012) and North Korea (Peng et al., 2011b). Therefore, the above weighted mean $^{207}Pb/^{206}Pb$ age of 923 ± 22 Ma reflects the crystallization age of the diabase sills emplaced into the Qiaotou Formations.

Eighteen spots on 18 zircon grains from sample 11210-1 emplaced into the Xingmincun Formation were analyzed (Fig. 9B). One concordant analysis (spot 01) yields a slightly older $^{207}Pb/^{206}Pb$ age of 1080 ± 45 Ma and reflected the age of the Mesoproterozoic inherited zircons. Apart from other 8 analyses (spots 02, 03, 05, 08, 10, 12, 14 and 15) with significant Pb loss, the remaining analyses yield a weighted mean $^{207}Pb/^{206}Pb$ age of 900 ± 34 Ma (95% confidence, MSWD = 1.9, N = 9). Their zircons are quite homogeneous and exhibit weak oscillatory zoning in CL images (Fig. 7B) with high contents of Th and U and high Th/U ratios (1.30–3.02, Table 1), typical of synmagmatic zircons from diabase samples. Therefore, the weighted mean $^{207}Pb/^{206}Pb$ age of 900 ± 34 Ma is interpreted as the crystallization age of the diabase sills emplaced into the Xingmincun Formation.

Eighteen spots on 18 zircon grains from sample 11205-1 emplaced into the Cuijiatun and Xingmincun Formations were dated and plotted on a concordia diagram in Fig. 9C. One analysis (spot 09) yields an early Paleoproterozoic inherited $^{207}Pb/^{206}Pb$ age of 2431 ± 20 Ma, similar to the ages of the basement rocks in the NCC. Two analyses (spots 10 and 14) yield Mesoproterozoic inherited $^{207}Pb/^{206}Pb$ age of 1309 ± 36 Ma and 1183 ± 29 Ma, respectively. Apart from 3 inherited analyses (spots 09, 10 and 14) and 7 analyses with significant Pb loss (spots 03, 05, 06, 13, 15, 16 and 17), the weighted mean $^{207}Pb/^{206}Pb$ age of the remaining analyses is 924 ± 28 Ma (95% confidence, MSWD = 1.5, N = 8, Fig. 9C). Similar to synmagmatic zircons from other samples, zircons from

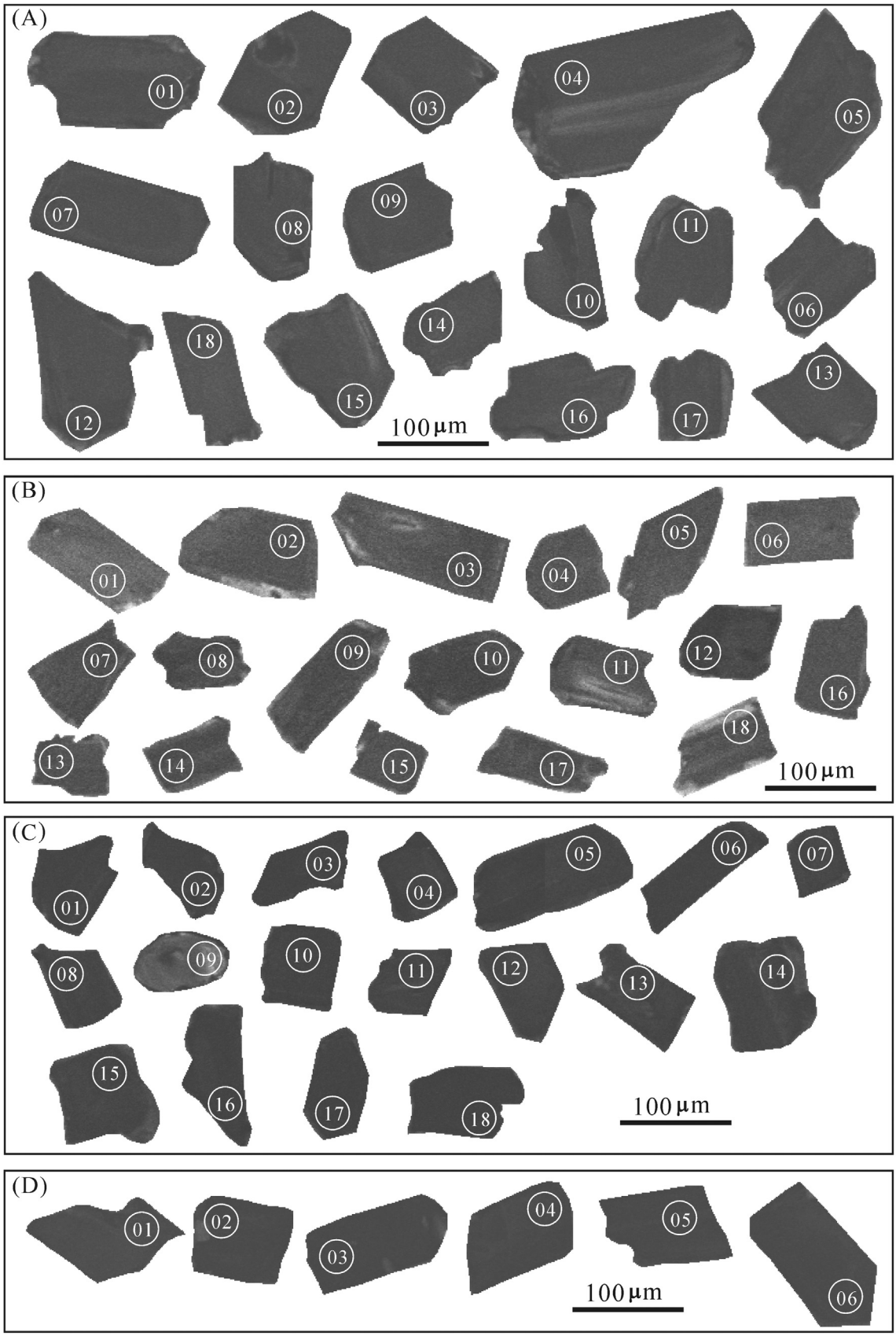

Fig. 7. CL images of the analyzed zircon grains together with LA-ICP-MS U–Pb analyses spots. (A) Sample 11224-1; (B) sample 11210-1; (C) sample 11205-1; (D) sample 11202-1.

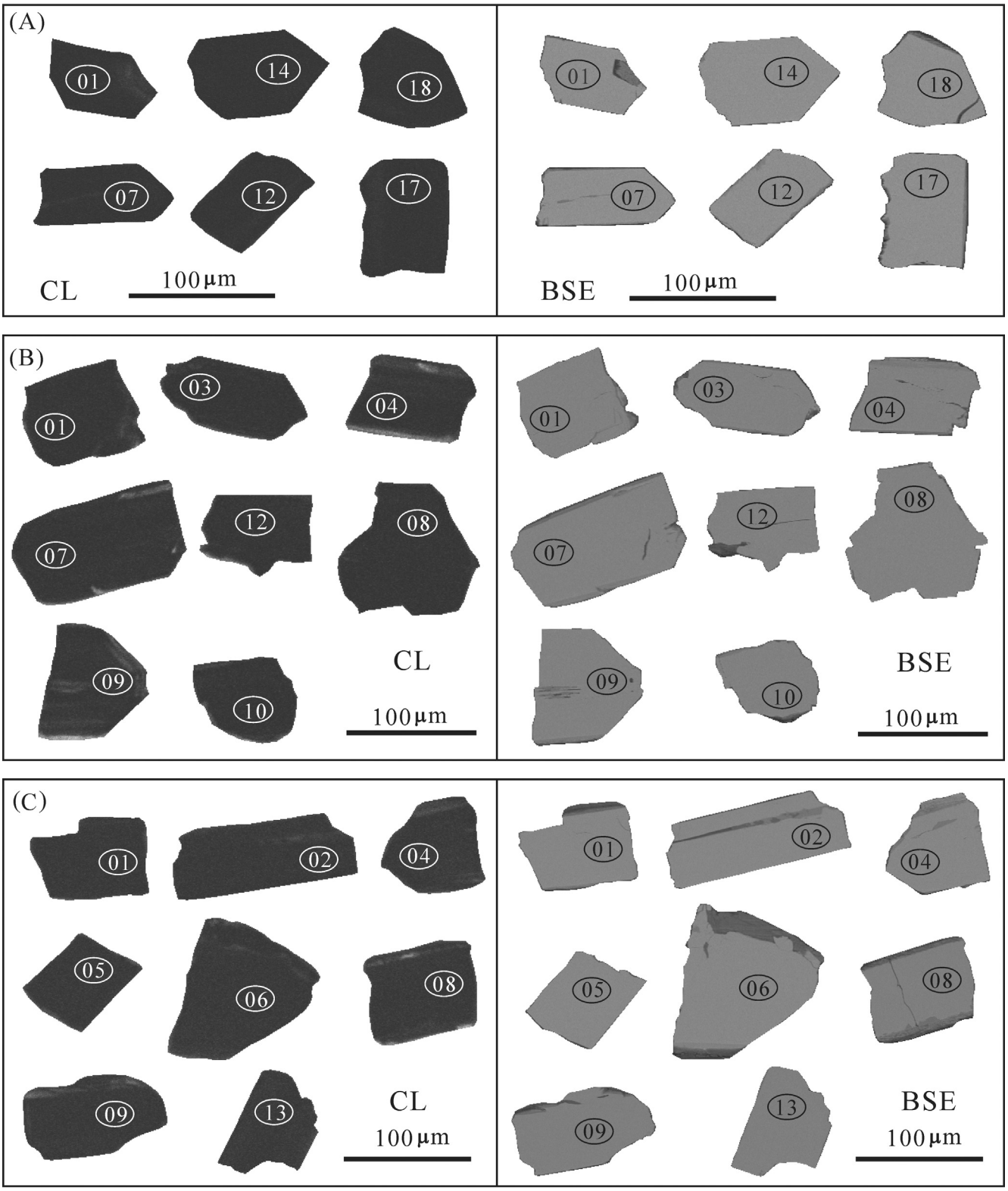

Fig. 8. CL and BSE images of the analyzed baddeleyite grains together with SIMS Pb–Pb analyses spots. (A) Sample 11205-1; (B) sample 11210-1; (C) sample 11217-1.

sample 11205-1 are quite homogeneous and exhibit weak oscillatory zoning in CL images (Fig. 7C) and show high contents of Th and U and high Th/U ratios (0.99–1.72, Table 1). Therefore, the weighted mean $^{207}Pb/^{206}Pb$ age of 924 ± 28 Ma is interpreted as the crystallization age of the diabase sills emplaced into the Cuijiatun and Xingmincun Formations.

Because most of zircons from sample 11202-1 emplaced into the Cuijiatun and Xingmincun Formations are characterized by significant Pb loss, only 6 spots on 6 grains were analyzed. One analyses (spot 01) with relatively low content of U (358 ppm) is concordant and yields a reliable $^{207}Pb/^{206}Pb$ age of 922 ± 46 Ma (Fig. 9D). Their zircons are also typical of synmagmatic zircons from diabase

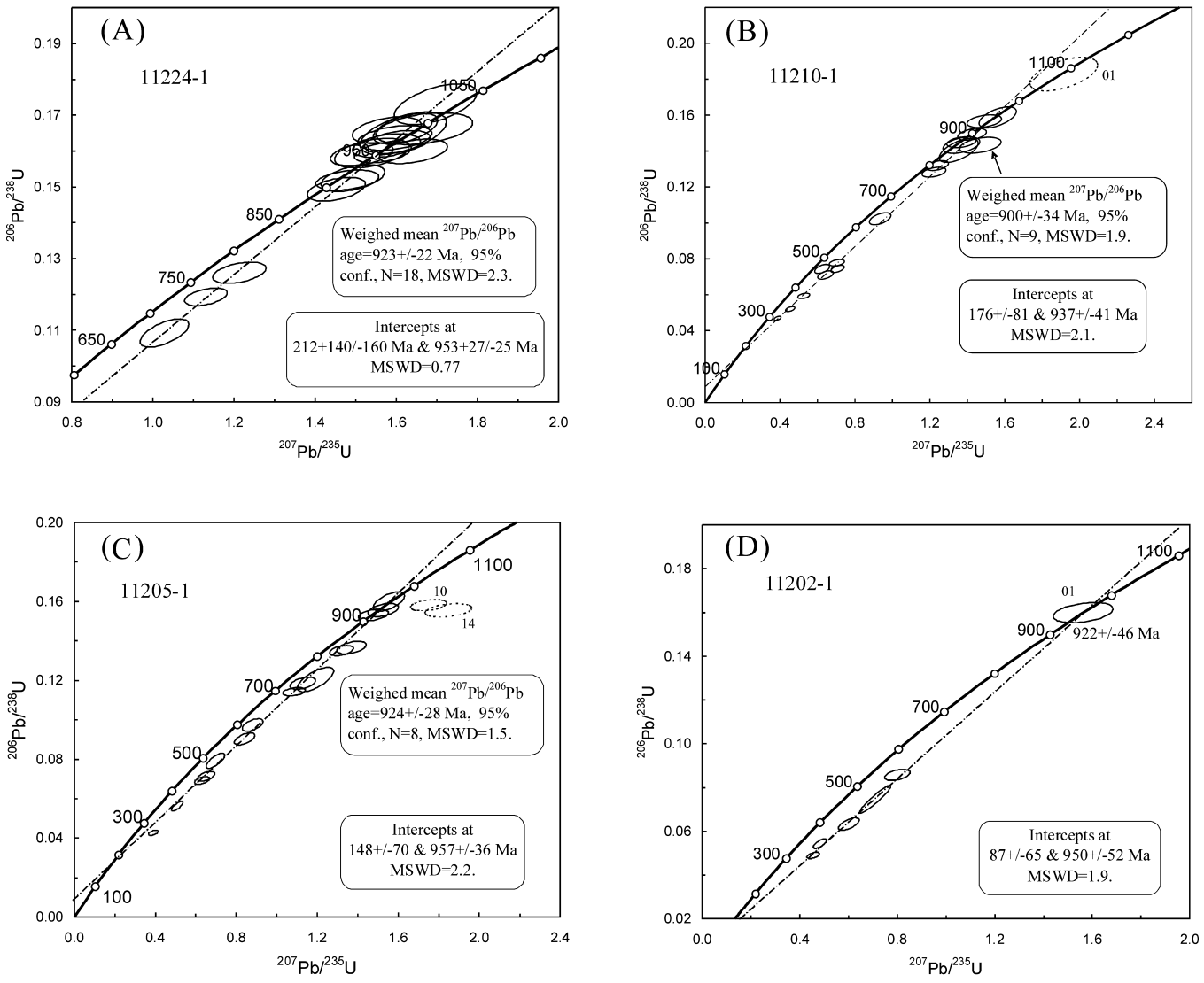

Fig. 9. U–Pb concordia diagrams for zircons from the diabase sill samples emplaced into the Neoproterozoic sedimentary rocks in the Liaodong Peninsula. Data-point error crosses are 2σ.

samples and exhibit weak oscillatory zoning in CL images (Fig. 7D) with high Th/U ratios of 1.09–3.93 (Table 1). Therefore, the $^{207}Pb/^{206}Pb$ age of 922 ± 46 Ma on the concordant analysis is interpreted as the crystallization age of the diabase sills emplaced into the Cuijiatun and Xingmincun Formations.

5.2. Baddeleyite Pb–Pb geochronology

Baddeleyites from three diabase samples were analyzed using the SIMS method and the analytical results are listed in Table 2 and plotted on $^{207}Pb/^{206}Pb$ age diagrams in Fig. 10. Twenty-one spots on 21 baddeleyite grains from sample 11205-1 emplaced into the Cuijiatun and Xingmincun Formations were dated and plotted on a $^{207}Pb/^{206}Pb$ age diagram in Fig. 10A. Except for three imprecise analyses due to high common Pb (spots 02, 03 and 09), the remaining analyses yield a weighted mean $^{207}Pb/^{206}Pb$ age of 924 ± 5 Ma (95% confidence, MSWD = 1.3, N = 18). This age is exactly the same as that of zircons from this sample (Fig. 9C), indicating emplacement of the diabase sills at *ca.* 0.92 Ga.

Nineteen spots on 19 baddeleyite grains from sample 11210-1 emplaced into the Xingmincun Formation were analyzed and plotted on a $^{207}Pb/^{206}Pb$ age diagram in Fig. 10B. Except for one analysis due to high common Pb (spot 02), the remaining analyses yield a weighted mean $^{207}Pb/^{206}Pb$ age of 886 ± 5 Ma (95% confidence, MSWD = 1.2, N = 18). The above age is similar to that of zircons from this sample (Fig. 9B), indicating emplacement of the diabase sills at 0.90–0.89 Ga.

Nineteen spots on 19 baddeleyite grains from sample 11217-1 emplaced into the Qiaotou Formation were analyzed and plotted on a $^{207}Pb/^{206}Pb$ age diagram in Fig. 10C. Except for one analysis due to high common Pb (spot 03), the remaining analyses yield a weighted mean $^{207}Pb/^{206}Pb$ age of 909 ± 7 Ma (95% confidence, MSWD = 1.4, N = 18), which is interpreted as the crystallization age of the diabase sills emplaced into the Qiaotou Formation at *ca.* 0.91 Ga.

5.3. Major and trace element compositions

The major and trace element compositions of 18 diabase sill samples emplaced into different layers within the Neoproterozoic strata in the Liaodong Peninsula are listed in Table 3. Most of them exhibit similar major and trace element compositions and are characterized by low contents of SiO_2 (45.62–54.77 wt.%) and K_2O (0.04–1.91 wt.%), high contents of TiO_2 (1.60–4.70 wt.%),

Table 2
SIMS Pb–Pb dating results of baddeleyites from the diabase sill swarms in the Liaodong Peninsula.

Grain spot	U (ppm)	$^{206}Pb/^{204}Pb$	$^{207}Pb^*/^{206}Pb^*$	±1σ (%)	$^{207}Pb^*/^{206}Pb^*$ Age (Ma)	±1σ
Sample 11205-1 (Liaodong Peninsula, diabase sills emplaced into the Cuijiatun and Xingmincun Formations; GPS position: E121°31.11′; N39°01.75′)						
11205-1@01	722	71265	0.06983	0.62	918	13
11205-1@02	381	519	0.09543	1.24	863	47
11205-1@03	273	556	0.09917	11.21	1029	428
11205-1@04	787	20364	0.07145	0.33	950	7
11205-1@05	1410	242825	0.06922	0.65	904	13
11205-1@06	740	67361	0.07000	0.32	922	7
11205-1@07	232	58272	0.07063	0.76	940	16
11205-1@08	996	47403	0.07012	0.61	923	13
11205-1@09	487	121	0.18086	3.85	645	403
11205-1@10	539	8992	0.07135	0.45	921	14
11205-1@11	1310	8101	0.07154	0.68	922	14
11205-1@12	862	114066	0.06951	0.73	910	15
11205-1@13	623	9174	0.07139	0.39	923	9
11205-1@14	1042	402178	0.06991	0.28	925	6
11205-1@15	318	1874	0.07802	0.78	940	30
11205-1@16	294	35544	0.07020	0.45	922	10
11205-1@17	1987	323803	0.06984	0.38	922	8
11205-1@18	1006	125703	0.06982	0.35	920	7
11205-1@19	273	20051	0.07042	0.50	920	11
11205-1@20	291	60059	0.06987	0.51	917	11
11205-1@21	486	4400	0.07252	0.48	907	14
Sample 11210-1 (Liaodong Peninsula, diabase sills emplaced into the Xingmincun Formations, GSP position: E121°53.27′; N39°02.59′)						
11210-1@01	872	8023	0.07060	0.70	893	18
11210-1@02	564	1146	0.08161	8.03	902	270
11210-1@03	1028	16470	0.06929	0.37	881	8
11210-1@04	1954	212567	0.06854	0.14	883	3
11210-1@05	735	75860	0.06915	0.26	898	6
11210-1@06	1320	141048	0.06911	0.55	899	11
11210-1@07	447	73855	0.07016	1.79	927	37
11210-1@08	969	122732	0.06899	0.42	895	9
11210-1@09	290	56299	0.06876	0.54	884	11
11210-1@10	2521	290015	0.06850	1.58	882	33
11210-1@11	263	40232	0.06853	0.38	874	8
11210-1@12	701	95715	0.06965	0.74	914	15
11210-1@13	1187	117102	0.06862	1.54	884	32
11210-1@14	1459	142032	0.06858	0.36	883	7
11210-1@15	2356	265442	0.06846	0.59	881	12
11210-1@16	1048	127698	0.06796	0.68	864	14
11210-1@17	1198	166161	0.06931	0.56	905	12
11210-1@18	327	41677	0.06874	0.57	881	12
11210-1@19	729	110385	0.06870	0.55	886	11
Sample 11217-1 (Liaodong Peninsula, diabase sills emplaced into the Qiaotou Formation, GSP position: E121°49.68′; N38°59.71′)						
11217-1@01	845	102650	0.06903	0.40	896	8
11217-1@02	724	98522	0.06955	0.67	911	14
11217-1@03	985	383	0.10897	7.78	975	357
11217-1@04	522	60535	0.06882	0.87	886	18
11217-1@05	833	81930	0.06924	0.77	901	16
11217-1@06	1347	167800	0.06895	0.71	895	15
11217-1@07	776	1740	0.07785	0.95	917	23
11217-1@08	2462	260118	0.06975	0.45	919	9
11217-1@09	2559	342765	0.06999	0.30	927	6
11217-1@10	670	63981	0.06986	0.73	918	15
11217-1@11	797	166728	0.06877	0.65	889	13
11217-1@12	3141	95988	0.06969	0.60	915	12
11217-1@13	4804	442517	0.06958	0.70	915	14
11217-1@14	455	1425	0.08001	2.23	927	68
11217-1@15	2091	4427	0.07016	2.02	835	53
11217-1@16	2338	77089	0.06950	0.25	908	6
11217-1@17	1190	155289	0.06859	1.16	884	24
11217-1@18	2055	241643	0.07000	1.26	927	26
11217-1@19	1333	147315	0.06896	0.49	895	10

Common Pb corrected using measured ^{204}Pb.

Fe_2O_3T (11.38–20.35 wt.%) and MgO (1.26–6.71 wt.%) and variable Mg# values from 14.9 to 53.9. In the total alkali ($K_2O + Na_2O$) vs. silica (SiO_2) and Nb/Y vs. Zr/TiO_2 classification diagrams (Fig. 11A, B), most of them fall into the fields of basalt and basaltic andesite and the subalkaline field. On the whole-rock alkali ($Na_2O + K_2O$)–FeOT–MgO (AFM) diagram for further classification of subalkaline volcanic rocks, they exhibit tholeiitic compositions (Fig. 11C). They exhibit similar rare earth element (REE) compositions with total REE contents from 54.9 ppm to 256.8 ppm. Their chondrite-normalized REE patterns (Fig. 12A, C, E) are characterized by slight light REE (LREE)-enrichment (La_N/Yb_N = 2.55–5.76) and no Eu anomalies (Eu_N/Eu_N = 0.82–1.22). On primitive mantle-normalized spidergrams (Fig. 12B, D, F), most of them are enriched in Rb, Ba, Th, U and light REE. They are also enriched in high field strength element (HFSE) and lack negative Nb, Ta, Zr, Hf, P and Ti anomalies.

Table 3
Major and trace element compositions of the diabase sill swarms in the Liaodong Peninsula.

Number	11197-1	11199-1	11200-1	11202-1	11203-1	11205-1	11206-1	11207-1	11210-1
Longitude	121°55.69′	121°35.35′	121°35.16′	121°32.02′	121°31.69′	121°31.11′	121°34.66′	121°30.70′	121°53.27′
Latitude	39°03.14′	39°03.55′	39°03.23′	39°02.41′	39°02.76′	39°01.75′	39°01.92′	39°00.71′	39°02.59′
Major element oxides (wt.%)									
SiO_2	48.17	50.56	47.44	49.15	47.92	54.77	50.93	49.73	45.62
TiO_2	2.56	2.25	3.83	4.23	4.05	2.17	3.71	3.19	4.06
Al_2O_3	13.01	13.42	11.80	11.90	12.16	12.34	11.98	12.37	13.14
Fe_2O_3T	14.47	12.71	18.19	16.67	17.43	14.30	17.01	14.79	16.90
MnO	0.21	0.19	0.24	0.21	0.19	0.14	0.24	0.20	0.21
MgO	5.26	5.37	4.70	3.50	3.82	1.26	3.27	5.37	4.97
CaO	8.35	10.14	8.52	6.95	5.98	2.92	6.28	8.55	9.52
Na_2O	1.88	2.44	2.29	2.59	3.04	2.57	2.75	2.85	2.46
K_2O	0.72	0.77	0.73	1.38	0.71	1.91	0.84	0.81	1.37
P_2O_5	0.23	0.24	0.30	0.57	0.42	0.79	0.42	0.32	0.29
LOI	5.05	1.89	1.95	2.81	4.25	6.78	2.58	1.78	1.44
Total	99.91	99.97	99.99	99.96	99.96	99.94	100.00	99.95	99.98
FeO	5.51	9.11	7.83	5.47	8.95	2.15	10.39	11.00	5.01
Mg#	41.9	45.6	33.9	29.4	30.3	14.9	27.6	41.8	36.8
Trace elements (ppm)									
La	11.4	14.0	16.3	32.5	22.1	41.9	24.8	24.3	20.2
Ce	28.2	34.9	38.2	68.3	48.9	88.2	57.2	55.1	44.3
Pr	3.95	4.83	5.25	9.25	6.90	12.3	7.78	7.15	5.69
Nd	18.4	22.3	24.2	40.6	30.9	53.6	35.4	30.9	24.6
Sm	5.08	5.80	6.47	9.84	7.69	12.5	9.27	7.12	5.85
Eu	1.79	1.97	2.33	3.22	2.73	3.78	3.05	2.08	2.13
Gd	5.24	6.49	7.01	10.2	8.42	13.1	10.0	6.97	5.90
Tb	0.88	1.08	1.16	1.57	1.38	2.10	1.59	1.11	0.97
Dy	5.58	6.54	6.87	9.47	8.42	12.6	9.94	6.64	5.73
Ho	1.10	1.28	1.40	1.82	1.65	2.47	1.95	1.27	1.10
Er	2.96	3.56	3.85	4.97	4.61	6.57	5.30	3.33	3.01
Tm	0.44	0.51	0.56	0.70	0.65	0.93	0.78	0.47	0.43
Yb	2.68	3.11	3.33	4.37	3.96	5.81	4.66	2.85	2.66
Lu	0.39	0.47	0.50	0.63	0.58	0.85	0.69	0.41	0.39
$\sum$REE	88.1	106.9	117.5	197.5	148.9	256.8	172.5	149.7	123.0
La_N/Yb_N	2.87	3.05	3.32	5.03	3.77	4.87	3.60	5.76	5.14
Eu_N/Eu_N^*	1.06	0.98	1.06	0.98	1.04	0.90	0.97	0.90	1.11
Li	15.0	19.6	24.1	24.0	22.3	17.2	20.2	18.8	15.5
Be	0.85	1.00	1.09	1.82	1.33	2.56	1.47	1.37	0.95
Sc	37.4	43.2	39.1	32.6	32.5	18.3	35.8	31.9	43.9
V	368	357	546	424	406	45.9	254	340	692
Cr	117	49.0	1.40	7.83	42.3	0.56	0.53	52.4	18.1
Co	45.2	43.7	48.3	39.3	40.4	16.9	37.8	48.6	52.7
Ni	69.4	39.2	16.8	21.3	36.3	0.51	0.76	49.4	48.6
Cu	53.5	32.8	43.8	32.0	26.1	7.09	5.83	150	223
Zn	100	96.8	125	197	109	138	137	232	141
Ga	19.4	21.8	22.4	22.6	21.9	25.0	24.2	18.5	23.0
Rb	18.4	21.5	19.0	46.0	28.5	62.1	21.2	15.8	47.6
Sr	357	305	219	336	432	198	199	285	359
Y	29.7	36.1	38.0	50.3	45.8	65.4	52.6	34.2	30.3
Zr	130	157	173	261	223	424	256	215	150
Nb	12.6	13.5	16.3	28.5	23.4	31.5	26.3	28.4	23.3
Sn	1.34	1.36	1.72	2.44	2.69	1.66	2.34	1.76	1.52
Cs	0.83	0.49	1.11	1.53	1.23	1.88	1.12	0.62	1.94
Ba	188	171	116	401	161	377	138	186	326
Hf	3.38	4.05	4.47	6.56	5.76	10.6	6.65	5.44	3.77
Ta	0.77	0.84	0.98	1.69	1.32	1.68	1.49	1.65	1.31
Tl	0.060	0.063	0.097	0.22	0.13	0.25	0.086	0.072	0.17
Pb	3.17	2.22	2.62	14.1	1.48	7.10	1.30	4.54	4.91
Th	1.85	2.26	2.36	5.55	3.63	9.91	3.57	3.91	2.06
U	0.41	0.46	0.52	1.23	0.78	1.98	0.76	0.91	0.44

Number	11213-1	11215-1	11217-1	11218-1	11220-1	11221-1	11223-2	11224-1	11227-1
Longitude	121°53.50′	121°53.37′	121°49.68′	121°40.47′	121°40.91′	121°28.90′	121°47.75′	121°48.05′	121°47.00′
Latitude	39°01.88′	39°01.98′	38°59.71′	38°54.25′	38°54.19′	38°57.70′	39°26.10′	39°26.22′	39°27.00′
Major element oxides (wt.%)									
SiO_2	47.52	46.88	48.24	47.35	48.28	46.84	46.24	47.89	51.93
TiO_2	1.60	1.97	3.28	2.76	2.87	2.75	4.70	2.49	2.93
Al_2O_3	14.38	13.57	12.55	14.24	14.68	13.12	14.45	13.86	12.21
Fe_2O_3T	11.38	13.08	16.55	13.78	16.08	14.21	20.35	13.46	16.93
MnO	0.16	0.18	0.22	0.17	0.20	0.20	0.22	0.18	0.25
MgO	6.71	5.15	4.32	4.65	5.88	6.34	2.46	6.21	2.89
CaO	10.56	10.21	8.84	9.12	7.23	8.88	2.21	10.06	4.57
Na_2O	2.22	2.63	2.43	1.93	1.92	1.87	1.30	1.96	2.54
K_2O	0.71	0.48	1.04	0.69	0.04	1.06	1.89	0.69	1.15
P_2O_5	0.14	0.19	0.45	0.28	0.37	0.28	0.60	0.25	0.62

Table 3 (*Continued*)

Number	11213-1	11215-1	11217-1	11218-1	11220-1	11221-1	11223-2	11224-1	11227-1
Longitude	121°53.50′	121°53.37′	121°49.68′	121°40.47′	121°40.91′	121°28.90′	121°47.75′	121°48.05′	121°47.00′
Latitude	39°01.88′	39°01.98′	38°59.71′	38°54.25′	38°54.19′	38°57.70′	39°26.10′	39°26.22′	39°27.00′
LOI	4.57	5.63	2.06	4.93	2.40	4.38	5.31	2.94	3.94
Total	99.95	99.96	99.98	99.90	99.94	99.93	99.73	99.99	99.96
FeO	4.84	3.98	4.37	5.04	9.44	9.22	4.44	5.11	8.76
Mg#	53.9	43.8	34.1	40.1	42.0	46.9	19.3	47.8	25.3
Trace elements (ppm)									
La	7.04	9.42	25.4	14.9	12.3	19.7	22.5	14.9	29.7
Ce	16.5	23.4	56.2	32.6	29.5	43.3	64.7	37.0	66.4
Pr	2.45	3.24	7.41	4.85	4.19	5.75	7.19	4.98	9.16
Nd	11.3	14.7	32.8	22.0	19.3	25.5	32.8	22.7	41.1
Sm	3.10	3.96	7.93	5.70	5.02	6.26	8.53	5.94	10.4
Eu	1.33	1.64	2.83	1.99	1.76	2.25	2.43	2.19	3.41
Gd	3.60	4.39	8.29	6.27	5.65	6.61	9.63	6.26	11.1
Tb	0.59	0.74	1.36	1.02	0.90	1.10	1.59	1.04	1.75
Dy	3.66	4.53	8.11	6.22	5.40	6.50	9.65	6.46	10.7
Ho	0.76	0.93	1.64	1.24	1.07	1.29	1.97	1.27	2.14
Er	2.05	2.65	4.45	3.39	3.03	3.57	5.40	3.44	5.91
Tm	0.31	0.35	0.64	0.47	0.42	0.51	0.77	0.48	0.84
Yb	1.86	2.23	3.95	2.84	2.62	3.05	4.69	3.08	5.38
Lu	0.27	0.32	0.59	0.43	0.37	0.46	0.71	0.44	0.80
$\sum$REE	54.9	72.6	161.5	103.9	91.5	125.9	172.6	110.2	198.9
La_N/Yb_N	2.55	2.85	4.34	3.53	3.17	4.36	3.25	3.28	3.73
Eu_N/Eu_N^*	1.22	1.20	1.07	1.02	1.01	1.07	0.82	1.10	0.97
Li	27.2	17.7	10.2	13.6	15.4	56.0	28.9	25.3	21.6
Be	0.43	0.52	1.21	0.92	0.82	1.03	1.85	1.10	1.99
Sc	39.9	36.7	37.9	36.8	35.3	38.1	37.8	35.2	25.7
V	289	312	344	354	331	340	302	367	148
Cr	239	83.2	6.84	262	268	68.9	5.14	155	0.67
Co	49.1	57.9	43.9	39.0	38.6	51.0	35.9	48.0	25.3
Ni	101	65.7	29.9	74.2	67.0	68.3	13.3	84.4	0.67
Cu	78.0	90.4	118	35.9	33.5	116	14.6	25.8	5.83
Zn	72.2	77.5	121	104	99.5	118	135	112	113
Ga	16.8	19.0	23.1	21.2	19.4	21.6	25.9	21.3	25.6
Rb	38.8	22.8	28.1	20.8	21.6	0.36	55.3	33.9	36.6
Sr	485	379	285	262	239	634	155	297	244
Y	20.9	24.8	43.9	33.9	28.9	34.2	51.2	34.0	57.7
Zr	70.6	89.8	209	148	130	159	262	163	323
Nb	5.90	7.38	23.0	14.4	12.1	15.9	3.82	15.3	32.8
Sn	0.75	0.87	1.80	1.42	1.28	1.38	2.48	1.69	3.93
Cs	1.22	1.06	4.66	0.57	0.68	0.14	1.48	0.89	1.03
Ba	351	128	328	172	414	30.8	657	431	295
Hf	1.91	2.39	5.22	3.81	3.27	4.09	6.84	4.18	8.04
Ta	0.37	0.45	1.23	0.88	0.73	0.96	0.12	0.93	1.73
Tl	0.12	0.086	0.18	0.17	0.15	0.004	0.36	0.24	0.25
Pb	1.15	5.38	4.83	2.94	4.30	4.13	2.61	2.22	1.55
Th	0.64	0.85	2.61	2.25	2.01	2.02	4.48	2.43	4.79
U	0.15	0.21	0.57	0.45	0.45	0.41	2.32	0.51	1.06

Fe_2O_3T – Fe_2O_3 total; LOI – loss on ignition; Mg# = molecular MgO/(TFeO + MgO); Eu_N – chondrite-normalized Eu; $Eu_N^* = (Sm_N \times Gd_N)^{1/2}$.

6. Discussion

6.1. Precise emplacement ages of the diabase sills in the Liaodong Peninsula

The emplacement ages of the diabase sills within the Neoproterozoic sedimentary rocks in the Liaodong Peninsula (named as the Dalian mafic sill swarms) are highly controversial. Although some researchers proposed their emplacement during the latest Mesoproterozoic to earliest Neoproterozoic (Liu et al., 2006; Peng et al., 2011b), others favor their emplacement during the Late Triassic (Yang et al., 2004, 2007b; Liu et al., 2013), or even the latest Neoarchean to earliest Paleoproterozoic (Liu et al., 2012), mainly based on zircon U–Pb dating. Yang et al. (2004) dated a diabase sample from a sill emplaced into the Qiaotou Formation near Daheishan by the zircon SHRIMP U–Pb method and most zircons are earliest Neoproterozoic in age and yield a weighted mean $^{207}Pb/^{206}Pb$ age of 904 ± 15 Ma (N = 9), which was considered as age of inherited zircons. One zircon grain yields a Late Triassic age of 211 ± 2 Ma and was considered as the emplacement age of the diabase sills (Yang et al., 2004). Yang et al. (2007b) reported the zircon SHRIMP U–Pb ages (213 ± 5 Ma, N = 11, MSWD = 1.2) of another diabase sample from a dyke within the Late Triassic syenite in the southwestern edge of the Liaodong Peninsula (Fig. 1). However, since the diabase sample dated by Yang et al. (2007b) is from a dyke emplaced into the Late Triassic syenite with distinct petrological and geochemical compositions as the diabase sills within the Neoproterozoic sedimentary rocks, the above age of 213 ± 5 Ma couldn't reflect the emplacement ages of the diabase sills in the Liaodong Peninsula. Recently, Liu et al. (2012) reported two zircon LA-ICP-MS U–Pb ages of 2510 ± 18 Ma (N = 15, MSWD = 0.72) and 2476 ± 18 Ma (N = 8, MSWD = 1.7) from two diabase sills within the Neoproterozoic strata near Dalian harbor and considered them as latest Neoarchean to earliest Paleoproterozoic mafic dykes. Obviously, latest Neoarchean to earliest Paleoproterozoic ages obtained by Liu et al. (2012) reflect those of inherited zircons since these diabase sills were emplaced into the Neoproterozoic sedimentary rocks. Later, Liu et al. (2013) reported a zircon LA-ICP-MS U–Pb age of 210 ± 2 Ma (N = 12, MSWD = 0.11) from a diabase sill within the Ganjingzi Formation west to Gezhenbu along the western coast of

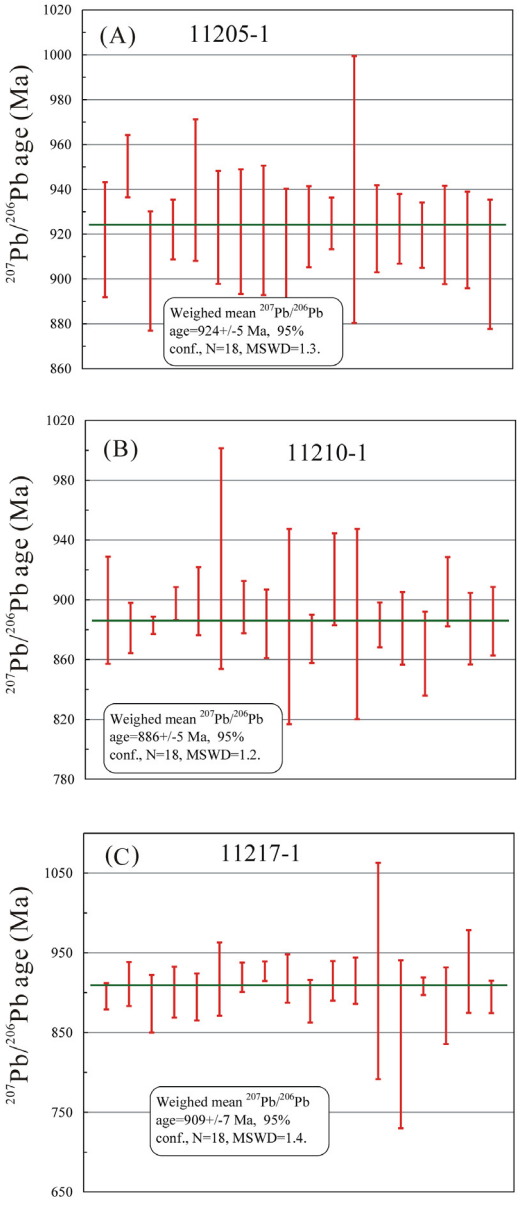

Fig. 10. $^{207}Pb/^{206}Pb$ age diagrams for baddeleyites from the diabase sill samples emplaced into the Neoproterozoic sedimentary rocks in the Liaodong Peninsula. Data-point error symbols are 2σ.

the Liaodong Peninsula. However, the *ca.* 210 Ma zircons dated by Liu et al. (2013) are characterized by strong oscillatory zoning (see Fig. 3 inset of Liu et al., 2013), which is very different from synmagmatic zircons separated from diabase samples (e.g., Liu et al., 2006; Gao et al., 2009; Zhang et al., 2009, 2012a; Peng et al., 2011b; Wang et al., 2012). Moreover, the Late Triassic emplacement ages of *ca.* 210 Ma are inconsistent with regional folding of these diabase sills with the hosting Neoproterozoic sedimentary rocks during the Middle-Late Triassic (e.g., Wang et al., 2000; GSILP, 2001; Yang et al., 2011), as indicated by the Yujiacun syenite pluton emplaced into the deformed Neoproterozoic strata in the southwestern edge of the Liaodong Peninsula with emplacement of 219 ± 1 Ma (Wu et al., 2005).

Our new zircon LA-ICP-MS U–Pb and baddeleyite SIMS Pb–Pb dating results on five samples from the diabase sills emplaced into the Neoproterozoic Qiaotou, Cuijiatun and Xingmincun Formations yields weighed mean $^{207}Pb/^{206}Pb$ ages from 924 ± 5 Ma to 886 ± 5 Ma, indicating emplacement of these diabase sill swarms during the early Neoproterozoic (Tonian) at *ca.* 920–890 Ma. Our synmagmatic zircons from the diabase samples exhibit similar characteristics (euhedral or subhedral prisms in shape, weak oscillatory zoning in CL images, high contents of Th and U and high Th/U ratios) as those of the Neoproterozoic zircons previously dated by Yang et al. (2004), indicating the Neoproterozoic zircons are synmagmatic zircons instead of inherited ones as previously reported (Yang et al., 2004). This is further confirmed by similar zircon U–Pb and baddeleyite Pb–Pb ages obtained by same samples (11210-1, Figs. 9B and 10B; 11205-1, Figs. 9C and 10A). Compared with zircon, baddeleyite ages are particularly useful in confirming the emplacement age of mafic-ultramafic rock, as baddeleyites are not inherited (e.g., Heaman and LeCheminant, 1993; Söderlund et al., 2013). The above newly obtained emplacement ages are consistent with the field occurrence of these diabase sills since they only occur within the Neoproterozoic sedimentary rocks and have never been found in the strata younger than the Neoproterozoic. Moreover, these Neoproterozoic emplacement ages are also consistent with the fact that the diabase sills were strongly deformed with the hosting Neoproterozoic sedimentary rocks prior to emplacement of the Yujiacun syenite pluton with zircon LA-ICP-MS U–Pb age of 219 ± 1 Ma (Wu et al., 2005).

6.2. Constraints on upper boundary of the Neoproterozoic strata and their macro- and microfossils in the southeastern NCC

Sedimentation of the Neoproterozoic strata in the Liaodong Peninsula has long been considered as from 1.00 Ga to 0.60 Ga or 0.54 Ga due to lack of reliable isotopic ages (e.g., LBGMR, 1989, 1997; Qiao and Gao, 2000; GSILP, 2001; Qiao, 2002; Meng and Ge, 2002; Wang et al., 2014b). Because the Xingmincun Formation in the topmost part of the Neoproterozoic strata in the Liaodong Peninsula was intruded by the Dalian diabase sills, our new zircon and baddeleyite ages provide important constraints on the upper boundary of the Neoproterozoic strata in the eastern NCC. Moreover, detrital zircon U–Pb dating on the Mesoproterozoic Yushulazi Formation overlain by the Yongning Formation in the lower most of the Neoproterozoic strata in the Liaodong Peninsula indicate its deposition after 1.05 Ga (Luo et al., 2006). Therefore, sedimentation of the extremely thick (>12.7 km) Neoproterozoic sedimentary rocks in the eastern NCC occurred during a short period from 1.05 Ga to 0.92–0.89 Ga. The sedimentary gap between the Neoproterozoic and Cambrian strata in the eastern NCC is longer than 0.35 Ga, which is much longer than previously regarded. The new geochronological results on diabase sills also indicate that the Liaodong Peninsula in the eastern NCC has undergone significant uplift prior to *ca.* 0.92–0.89 Ga. In the Xu-Huai area in the southeastern NCC, sedimentation of the Neoproterozoic strata had ended prior to *ca.* 0.92–0.89 Ga because the Jinshanzhai and Wangshan Formations in the topmost part of the Neoproterozoic strata were intruded by the early Neoproterozoic diabase sills (ABGMR, 1977; Pan et al., 2000a, 2000b; Liu et al., 2006; Wang et al., 2012). Therefore, sedimentation of the Neoproterozoic strata in the southeastern NCC had ended prior to *ca.* 0.92–0.89 Ga, which is much earlier than previously regarded (e.g., LBGMR, 1989, 1997; Qiao and Gao, 2000; GSILP, 2001; Meng and Ge, 2002).

Macroscopic carbonaceous fossils and organic-walled microfossils are very common in the Neoproterozoic strata of Xu-Huai (e.g., Sun et al., 1986; Zang and Walter, 1992; Yin and Sun, 1994; Dai et al., 2012; Tang et al., 2013, 2015; Xiao et al., 2014), eastern Shandong (e.g., Yin, 1991) and Liaodong Peninsula (e.g., Hong et al., 1988; Chen, 1990, 1991) in the eastern and southeastern NCC. They were named as "Huainan Biota" (e.g., Zheng, 1979; Niu and Zhu, 2002) and are comparable with the Precambrian biota from the Little Dal Group in the Mackenzie Mountains of northwestern Canada (e.g.,

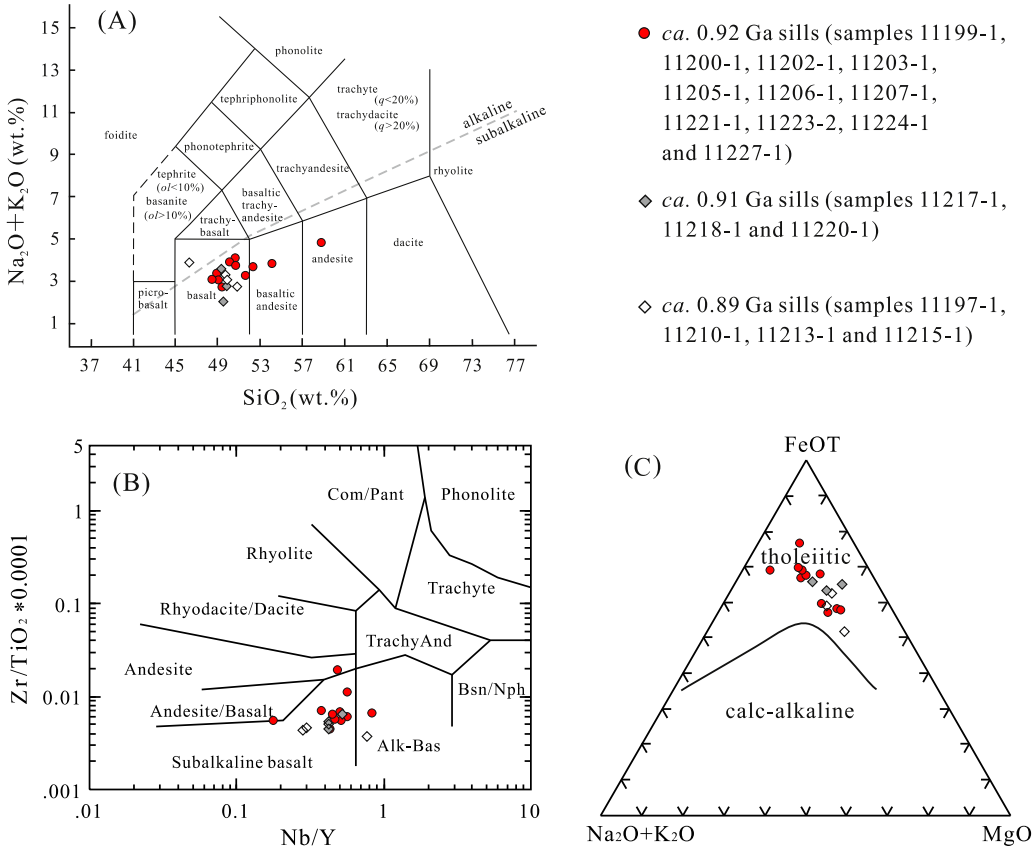

Fig. 11. (A) Total alkali ($K_2O + Na_2O$) vs. silica (SiO_2) (Le Bas et al., 1986), (B) Nb/Y vs. Zr/TiO_2 (Winchester and Floyd, 1977) and (C) whole-rock alkali ($Na_2O + K_2O$)–FeOT–MgO (AFM) (Irvine and Baragar, 1971) classification diagrams for the Dalian diabase sills within the Neoproterozoic sedimentary rocks in the Liaodong Peninsula.

Hofmann and Aitken, 1979). Although these fossils were considered as a special biota prior to the Neoproterozoic global glaciations (Snowball Earth) and are of great significance for early Neoproterozoic global biological evolution (e.g., Niu and Zhu, 2002; Xiao et al., 2014), their ages are highly controversial, mainly due to poor constraints on the ages of the Neoproterozoic strata in the eastern and southeastern NCC. Traditionally, the Neoproterozoic strata in the eastern and southeastern NCC and their fossils were regarded as Cryogenian–Ediacaran in age (e.g., Xing, 1989; Yin, 1991; Zang and Walter, 1992; Yin and Sun, 1994; Xing et al., 1996; Qiao and Gao, 2000; Qiao, 2002; Niu and Zhu, 2002; Liu et al., 2005a). However, recent results show that these fossils and the Neoproterozoic strata of Xu-Huai area are likely early Neoproterozoic (Tonian) in age (Tang et al., 2013, 2015; Xiao et al., 2014). Our new zircon U–Pb and baddeleyite Pb–Pb dating results of the diabase sills emplaced into the Neoproterozoic sedimentary rocks in the Liaodong Peninsula further confirmed that the Neoproterozoic strata and their fossils in the eastern and southeastern NCC are definitely Tonian in age.

6.3. Comparison with the Neoproterozoic mafic dykes and diabase sills in other parts of the NCC (Sino-Korean Craton)

Neoproterozoic magmatic events have seldom been reported in the NCC previously. Recently, some Neoproterozoic mafic magmatism was recognized from the central and eastern Sino-Korean Craton (Figs. 1 inset and 2, Liu et al., 2006; Gao et al., 2009; Peng et al., 2011a, 2011b; Wang et al., 2012). These include the Xu-Huai diabase sills in the southeastern NCC (zircon SHRIMP $^{206}Pb/^{238}U$ ages of 925 ± 10 Ma to 907 ± 38 Ma, recalculated from Liu et al., 2006; zircon SHRIMP $^{206}Pb/^{238}U$ age of 930 ± 10 Ma, Gao et al., 2009; zircon SHRIMP and LA-ICP-MS $^{206}Pb/^{238}U$ ages from 933 ± 14 Ma to 890 ± 14 Ma, Wang et al., 2012), the Dashigou mafic dykes in the central NCC (baddeleyite TIMS and SIMS $^{207}Pb/^{206}Pb$ ages from 926 ± 2 Ma to 920 ± 6 Ma, Peng et al., 2011a) and the Sariwon diabase sills in North Korea (baddeleyite SIMS $^{207}Pb/^{206}Pb$ age of 899 ± 7 Ma, Peng et al., 2011b). The newly obtained *ca.* 920–890 Ma emplacement ages of the Dalian diabase sills in the Liaodong Peninsula are similar to those of the Neoproterozoic mafic dykes and diabase sills in other parts of the Sino-Korean Craton, indicating emplacement of the mafic magmatism in the central and eastern Sino-Korean Craton during the early Neoproterozoic (Tonian) at around 0.92–0.89 Ga. The newly identified Dalian mafic sills, together with the Xu-Huai and Sariwon mafic sills and the Dashigou mafic dykes, constitute an early Neoproterozoic (0.92–0.89 Ga) large igneous province in the Sino-Korean Craton (Fig. 2).

The early Neoproterozoic diabase sills in the Liaodong Peninsula consist mainly of clinopyroxene, plagioclase and Fe-Ti oxides and belong to the tholeiitic series (Fig. 11, group 1 of Yang et al., 2007b; Liu et al., 2013). Their mineral assemblage and geochemical compositions are very similar to those of the recently recognized early Neoproterozoic Xu-Huai diabase sills in the southeastern NCC (Pan et al., 2000a; Wang et al., 2012), the Sariwon diabase sills in North Korea (Peng et al., 2011b) and the Dashigou mafic dykes in the central NCC (Peng et al., 2011a). If calculated using new emplacement age of 905 Ma, the diabase sills in the Liaodong Peninsula exhibit $\varepsilon_{Nd}(t)$ values of −0.9 to 4.5 and Nd isotopic T_{DM} model ages of 1.16–1.85 Ga (recalculated from Yang et al., 2007b and Liu et al., 2013). These Nd isotopic compositions are also similar to those of the Xu-Huai and Sariwon diabase sills and Dashigou mafic dykes (Peng et al., 2011a, 2011b), indicating all these sill (dyke) swarms could relate to same mantle processes during the early

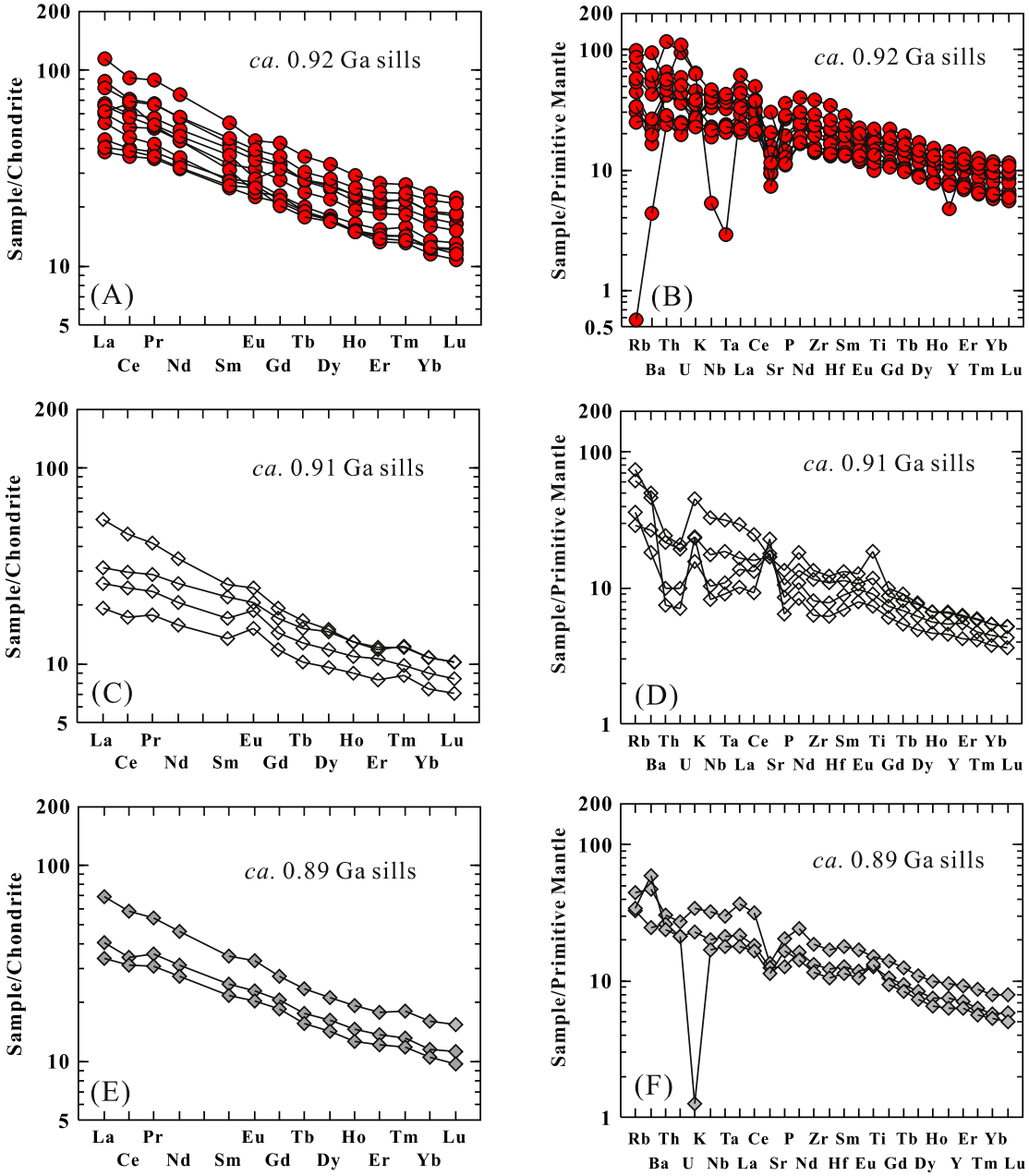

Fig. 12. Chondrite-normalized REE patterns (A, C, E) and primitive mantle-normalized spidergrams (B, D, F) for the Dalian diabase sills within the Neoproterozoic sedimentary rocks in the Liaodong Peninsula. The chondrite and primitive mantle values are from Taylor and McLennan (1985) and Sun and McDonough (1989), respectively. Symbols as in Fig. 11.

Neoproterozoic. Slightly negative to positive $\varepsilon_{Nd}(t)$ values and young Nd isotopic T_{DM} model ages indicate that ancient lithospheric mantle of the NCC was not main source areas of the early Neoproterozic diabase sill (dyke) swarms. On the Zr/Y vs. Zr and Ti–Zr–Y discrimination diagrams (Fig. 13), most diabase samples fall into the field of within plate basalt. Therefore, the 0.92–0.89 Ga diabase sill swarms in the Liaodong Peninsula were likely generated by partial melting of the depleted asthenosphere mantle coupled with differential crustal assimilation in a continental rifting setting that finally led to fragmentation of the southeastern NCC from the Rodinia supercontinent. Emplacement of the 0.92–0.89 Ga diabase sills from continental rifting to lithospheric rupture is also supported by their evolution trend from within plate basalt to mid-ocean ridge basalt on the Zr/Y vs. Zr discrimination diagram (Fig. 13A).

6.4. Early Neoproterozoic pre-magmatic regional uplift of the southeastern NCC

Pre-magmatic surface uplift is a very common process associated with large igneous provinces and mantle plumes (e.g., Campbell and Griffiths, 1990; Griffiths and Campbell, 1991; Rainbird, 1993; Farnetani and Richards, 1994; Williams and Gostin, 2000; Rainbird and Ernst, 2001; Sengör, 2001; Stephen et al., 2001; Nyblade and Sleep, 2003; He et al., 2003; Ernst and Buchan, 2003; Mazumder and Foulger, 2004; Trubitsyn and Trubitsyn, 2005; Campbell, 2005; Saunders et al., 2007; Ernst, 2014). Many major mafic/ultramafic lavas have been attributed to mantle plumes that are expected to produce crustal uplift (doming) preceding the major phase of volcanism (Mazumder and Foulger, 2004). Such pre-magmatic uplift would significantly affect regional

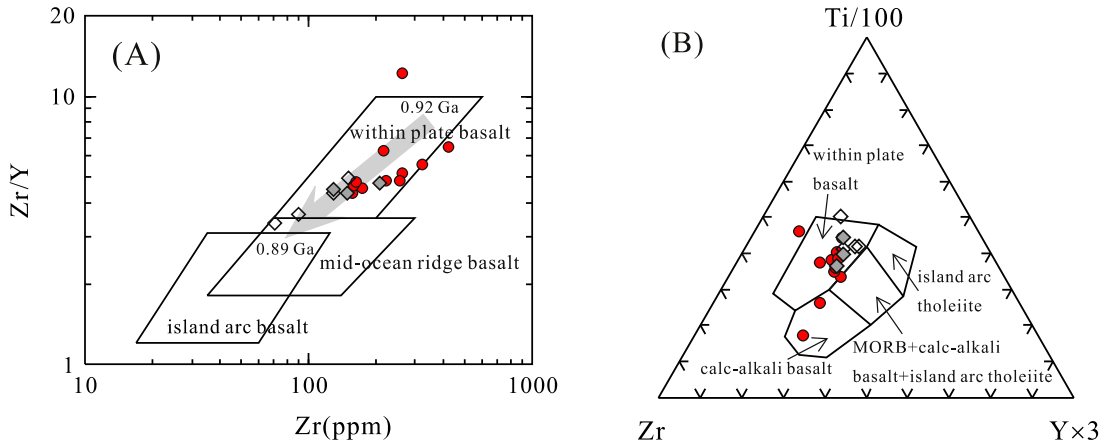

Fig. 13. Major and trace elements discrimination diagrams for the Dalian diabase sills within the Neoproterozoic sedimentary rocks in the Liaodong Peninsula. (A) Zr/Y vs. Zr diagram from Pearce and Norry (1979); (B) Ti–Zr–Y diagram from Pearce and Cann (1973). Symbols as in Fig. 11.

sedimentation patterns and lead to thinning or absence and erosion of strata (Rainbird, 1993; Rainbird and Ernst, 2001; He et al., 2003; Mazumder and Foulger, 2004). It is difficult to defend a large igneous province-mantle plume connection where pre-magmatic lithospheric uplift is absent (Mazumder and Foulger, 2004). Recent results have revealed that all rifts undergo a phase of uplift before the lithosphere ruptures (Esedo et al., 2012; Frizonde de Lamotte et al., 2015). Uplift of margins prior to breakup is typical, and an expected process accompanying continental breakup (Esedo et al., 2012). Pre-breakup uplift has been reported in the North Atlantic Igneous Province, the Main Ethiopian Rift, East Africa and the Iberia-Newfoundland rift system (Meyer et al., 2007; Corti, 2009; Péron-Pinvidic and Manatschal, 2009). Initial breakup of Gondwana in Antarctica was characterized by emplacement of *ca.* 180 Ma Ferrar diabase sill swarms and pre-magmatic uplift in the Transantarctic Mountains (e.g., Elliot and Fleming, 2000, 2008; Bédard et al., 2007). Therefore, recognizing of pre-magmatic uplift is very important to link mafic sill (dyke) swarms and lavas with mantle plume and/or continental breakup events.

Our field investigation and new geochronological results of the diabase sills emplaced into the Neoproterozoic sedimentary rocks in the Liaodong Peninsula (Fig. 2) indicate that sedimentation of the Neoproterozoic strata in the eastern NCC had ended prior to *ca.* 0.92–0.89 Ga. Similar absence of sedimentation of the Neoproterozoic strata occurred in Xu-Huai area in southeastern NCC as revealed by our field investigation and previously geochronological results (Liu et al., 2006; Gao et al., 2009; Wang et al., 2012). Therefore, the southeastern NCC has undergone significant uplift prior to *ca.* 0.92–0.89 Ga. The above pre-magmatic regional uplift is of significant tectonic implications and probably resulted from pre-breakup uplift (Esedo et al., 2012) related to breakup (from rifting to rupture) of the NCC from the Rodinia supercontinent. Pre-magmatic uplift of the southeastern NCC recognized in this contribution provides important evidence for continental rifting and initial breakup of the southeastern NCC from the Rodinia supercontinent in the early Neoproterozoic at around 0.92–0.89 Ga.

6.5. Tectonic implications for evolution of the NCC in the Rodinia supercontinent

Although reliable late Mesoproterozoic (1.2–1.0 Ga) tectonomagmatic records during assembly of the Rodinia supercontinent has not been reported in the NCC, abundant 1.2–1.0 Ga detrital zircons have been identified from the latest Mesoproterozoic to Neoproterozoic sedimentary rocks in the eastern and southeastern Sino-Korean Craton (Li et al., 2005; Luo et al., 2006; Gao et al., 2010; Chu et al., 2011; Lu et al., 2012; Yang et al., 2012; Hu et al., 2012). These 1.2–1.0 Ga detrital zircons were considered as evidence for assembly of the NCC within the Rodinia supercontinent (e.g., Lu et al., 2012), even though their source areas are still unclear. Existence of the 1.2–1.0 Ga detrital zircons and 0.92–0.89 Ga mafic magmatism in the eastern and southeastern NCC indicates that the southeastern margin of the NCC was probably connected to some other continents that are characterized by strong Grenville magmatism in the Rodinia supercontinent (Fig. 2). Continental rifting and initial breakup of the southeastern NCC from some other continents in the Rodinia supercontinent occurred in the early Neoproterozoic at around 0.92–0.89 Ga, which is much earlier than fragmentation of main components of the Rodinia supercontinent during the Mid-Neoproterozoic (e.g., Li et al., 2008). Fragmentation and break-up of the Rodinia supercontinent was likely diachronously.

Since ages of the early Neoproterozoic diabase sill (dyke) swarms in the Sino-Korean Craton are similar to those of the Gangil-Mayumbian bimodal volcanics in the Congo Craton (Tack et al., 2001; Ernst et al., 2008, 2013) and the Bahia mafic dykes in the São Francisco Craton (Evans et al., 2010, 2015), Peng et al. (2011a) and Cederberg et al. (2015) proposed that the NCC was probablly connected to Congo and São Francisco cratons in the Rodinia supercontinent. However, in many palaeomagnetic and paleogeographic reconstruction of the Rodinia supercontinent in the early Neproterozoic period (e.g., Zhai et al., 2003; Zhang et al., 2006; Li et al., 2008; Evans, 2009; Lu et al., 2012), the NCC was very far from the Congo and São Francisco cratons. Recent paleomagnetic results from the early Neoproterozoic mafic sills and carbonate rocks in the Xu-Huai area in the southeastern NCC suggest paleogeographic proximities of the NCC to Laurentia, and probably to Siberia as well in the supercontinent Rodinia (Fu et al., 2015). Although the early Neoproterozoic sill (dyke) swarms and pre-magmatic uplift of the southeastern NCC provide important evidence for breakup of the NCC from the Rodinia supercontinent, the position of the NCC within the Rodinia supercontinent is still uncertain. Further paleomagnetic studies on these newly identified early Neoproterozoic diabase sills in the Liaodong Peninsula will provide important constraints on the position of the NCC within the Rodinia supercontinent.

7. Conclusions

1) Our new zircon LA-ICP-MS U–Pb and baddeleyite Pb–Pb dating results on five samples from the Qiaotou, Cuijiatun and Xingmincun Formations clearly indicated that emplacement of the large volume of diabase sills (the Dalian mafic sill swarms) within

the Neoproterozoic sedimentary rocks in the Liaodong Peninsula occurred during the early Neoproterozoic (Tonian) at *ca.* 920–890 Ma, not Late Triassic or latest Neoarchean to earliest Paleoproterozoic as previously reported.

2) The age for the upper boundary of the Neoproterozoic strata (Xingmincun Formation) in the Liaodong Peninsula is no later than 0.92–0.89 Ga, which is much earlier than previously regarded. Sedimentation of the extremely thick Neoproterozoic sedimentary rocks in the eastern and southeastern NCC occurred during a short period from 1.05 Ga to 0.92–0.89 Ga. The Neoproterozoic strata and their macroscopic carbonaceous fossils and organic-walled microfossils in the eastern and southeastern NCC are definitely Tonian in age, not Cryogenian–Ediacaran age as previously suggested. The sedimentary gap between the Neoproterozoic and Cambrian strata in eastern and southeastern North China Craton could be much longer than previously regarded.
3) The southeastern NCC has undergone significant uplift prior to *ca.* 0.92–0.89 Ga. This pre-magmatic (or pre-breakup) uplift could be either related to a mantle plume or rifting leading to breakup of the southeastern NCC from the Rodinia supercontinent at 0.92–0.89 Ga.
4) Formation of the early Neoproterozoic diabase sill swarms in southeastern NCC is likely related to a continental rifting event leading to breakup of the southeastern NCC from some other continents in the Rodinia supercontinent at *ca.* 0.92–0.89 Ga, which is much earlier than fragmentation of main components of the Rodinia supercontinent during the Mid-Neoproterozoic peroid.

Acknowledgments

We thank X.H. Li, Q.L. Li, Y. Liu, J. Li, G.Q. Tang, Z.C. Hu, Y.S. Liu and X. Yan for their assistance during SIMS and LA-ICP-MS analyses and CL imaging. Thoughtful and constructive reviews by R.E. Ernst, S.W. Liu and G.C. Zhao (Editor-in-Chief) significantly improved the quality of the manuscript. This research was financially supported by the National Basic Research Program of China (2012CB416604) and the National Natural Science Foundation of China (40972149).

References

ABGMR (Anhui Bureau of Geology and Mineral Resources), 1977. Geological Map and Explanation of Dangshan (I-50-XV), Suxian (I-50-XXI), and Lingbi (I-50-XXII). Scale 1:200000 (in Chinese).

Bédard, J.H.J., Marsh, B.D., Hersum, T.G., Naslund, H.R., Mukasa, S.B., 2007. Large-scale mechanical redistribution of orthopyroxene and plagioclase in the basement sill, Ferrar dolerites, McMurdo Dry Valleys, Antarctica: petrological, mineral-chemical and field evidence for channelized movement of crystals and melt. J. Petrol. 48, 2289–2326.

Bing, Z., Wang, Z., 2004. Indosinian orogeny in the eastern margin of North China Platform: tectonic deformation in Dalian area. Acta Geosci. Sin. 25, 555–560 (in Chinese with English abstract).

Bleeker, W., Ernst, R., 2006. Short-lived mantle generated magmatic events and their dyke swarms: the key unlocking Earth's paleogeographic record back to 2.6 Ga. In: Hanski, E., Mertanen, S., Rämö, T., Vuollo, J. (Eds.), Dyke Swarms: Time Markers of Crustal Evolution. Taylor and Francis/Balkema, London, pp. 3–26.

Campbell, I.H., Griffiths, R.W., 1990. Implications of mantle plume structure for the evolution of flood basalts. Earth Planet. Sci. Lett. 99, 79–93.

Campbell, I.H., 2005. Large igneous provinces and the mantle plume hypothesis. Elements 1, 265–269.

Cederberg, J., Söderlund, U., Oliveira, E.P., Ernst, R.E., Pisarevsky, S.A., (in press) 2015. U–Pb Baddeleyite Dating of the Proterozoic Pará de Minas Dyke Swarm in the São Francisco Craton (Brazil) – Implications for Tectonic Correlation with Siberia, Congo and the North China Cratons. GFF.

Chen, M., 1990. Macrofossils from the Late Precambrian Nanguanling Formation of Wuhangshan Group on the southern Liaodong Peninsula. Sci. Geol. Sin. 25, 315–323 (in Chinese with English abstract).

Chen, M., 1991. Discussion on the stratigraphic significance of macrofossils from the Late Precambrian sequence in southern Liaoning Province. Sci. Geol. Sin. 26, 120–128 (in Chinese with English abstract).

Chen, L., Huang, B., Yi, Z., Zhao, J., Yan, Y., 2013. Paleomagnetism of ca. 1.35 Ga sills in northern North China Craton and implications for paleogeographic reconstruction of the Mesoproterozoic supercontinent. Precambrian Res. 228, 36–47.

Chu, H., Lu, S.N., Wang, H.C., Xiang, Z.Q., Liu, H., 2011. U–Pb age spectrum of detrital zircons from the Fuzikuang Formation, Penglai Group in Changdao, Shandong Province. Acta Petrol. Sin. 27, 1017–1028 (in Chinese with English abstract).

Corti, G., 2009. Continental rift evolution: from rift initiation to incipient break-up in the Main Ethiopian Rift, East Africa. Earth Sci. Rev. 96, 1–53.

Dai, Z., Yan, X., Yuan, X., Yin, L., 2012. New data on silicified Proterozoic microfossils from the Jiudingshan Formation of Jiangsu and northern Anhui, China. Acta Palaeontol. Sin. 51, 26–55 (in Chinese with English abstract).

Dalziel, I.W.D., 1991. Pacific margins of Laurentia and East Antarctica–Australia as a conjugate rift pair: evidence and implications for an Eocambrian supercontinent. Geology 19, 598–601.

Elliot, D.H., Fleming, T.H., 2000. Weddell triple junction: the principal focus of Ferrar and Karoo magmatism during initial breakup of Gondwana. Geology 28, 539–542.

Elliot, D.H., Fleming, T.H., 2008. Physical volcanology and geological relationships of the Jurassic Ferrar Large Igneous Province, Antarctica. J. Volcanol. Geotherm. Res. 172, 20–37.

Ernst, R.E., Head, J.W., Parfitt, E., Grosfils, E., Wilson, L., 1995. Giant radiating dyke swarms on earth and venus. Earth Sci. Rev. 39, 1–58.

Ernst, R.E., Buchan, K.L., 2003. Recognizing mantle plumes in the geological record. Ann. Rev. Earth Planet. Sci. 31, 469–523.

Ernst, R.E., Wingate, M.T.D., Buchan, K.L., Li, Z.X., 2008. Global record of 1600–700 Ma Large Igneous Provinces (LIPs): implications for the reconstruction of the proposed Nuna (Columbia) and Rodinia supercontinents. Precambrian Res. 160, 159–178.

Ernst, R.E., Bleeker, W., Söderlund, U., Kerr, A.C., 2013. Large Igneous Provinces and supercontinents: toward completing the plate tectonic revolution. Lithos 174, 1–14.

Ernst, R.E., 2014. Large Igneous Provinces. Cambridge University Press, Cambridge, United Kingdom, 653 p.

Esedo, R., van Wijk, J., Coblentz, D., Meyer, R., 2012. Uplift prior to continental breakup: indication for removal of mantle lithosphere? Geosphere 8, 1078–1085.

Evans, D.A.D., 2009. The palaeomagnetically viable, long-lived and all-inclusive Rodinia supercontinent reconstruction. In: Murphy, J.B., Keppie, J.D., Hynes, A.J. (Eds.), Ancient Orogens and Modern Analogues. Geological Society, London, pp. 371–404, Special Publications 327.

Evans, D.A.D., Heaman, L.M., Trindade, R.I.F., D'Agrella-Filho, M.S., Smirnov, A.V., Catelani, E.L., 2010. Precise U–Pb baddeleyite ages from Neoproterozoic mafic dykes in Bahia, Brazil, and their Paleomagnetic/Paleogeographic implications. In: AGU Brazil Abstract, GP31E-07 American Geophysical Union, Joint Assembly, Meeting of the Americas, Iguassu Falls, August 2010.

Evans, D.A.D., 2013. Reconstructing pre-Pangean supercontinents. Geol. Soc. Am. Bull. 125, 1735–1751.

Evans, D.A.D., Trindade, R.I.F., Catelani, E.L., D'Agrella-Filho, M.S., Heaman, L.M., Oliveira, E.P., Söderlund, U., Ernst, R.E., Smirnov, A.V., Salminen, J.M., 2015. Return to Rodinia? Moderate to high paleolatitude of the São Francisco/Congo craton at 920 Ma. In: Li, Z.X., Evans, D.A.D., Murphy, J.B. (Eds.), Supercontinent Cycles Through Earth History. Geological Society of London, http://dx.doi.org/10.1144/SP424.1, Special Publication 424.

Fahrig, W.F., 1987. The tectonic setting of continental mafic dyke swarms: failed arm and early passive margin. In: Halls, H.C., Fahrig, W.F. (Eds.), Mafic Dyke Swarms. Geological Association of Canada Special Paper 34, pp. 331–348.

Farnetani, C.G., Richards, M.A., 1994. Numerical investigations of the mantle plume initiation model for flood basalt events. J. Geophys. Res. 99 (B7), 13813–13833, http://dx.doi.org/10.1029/94JB00649.

Frizonde de Lamotte, D., Fourdan, B., Leleu, S., Leparmentier, F., de Clarens, P., 2015. Style of rifting and the stages of Pangea breakup. Tectonics 34, 1009–1029, http://dx.doi.org/10.1002/2014TC003760.

Fu, X., Zhang, S., Li, H., Ding, J., Li, H., Yang, T., Wu, H., Yuan, H., Lv, J., 2015. New paleomagnetic results from the Huaibei Group and Neoproterozoic mafic sills in the North China Craton and their paleogeographic implications. Precambrian Res. 269, 90–106.

Gao, L.Z., Zhang, C.H., Shi, X.Y., Zhou, H.R., Wang, Z.Q., 2007. Zircon SHRIMP U–Pb dating of the tuff bed in the Xiamaling Formation of the Qingbaikouan System in North China. Geol. Bull. China 26, 249–255 (in Chinese with English abstract).

Gao, L.Z., Zhang, C.H., Shi, X.Y., Song, B., Wang, Z.Q., Liu, Y.M., 2008. Mesoproterozoic age for Xiamaling Formation in North China Plate indicated by zircon SHRIMP dating. Chin. Sci. Bull. 53, 2665–2671.

Gao, L.Z., Zhang, C.H., Liu, P.J., Tang, F., Song, B., Ding, X.Z., 2009. Reclassification of the Meso- and Neoproterozoic chronostratigraphy of North China by SHRIMP zircon ages. Acta Geol. Sin. 83, 1074–1084 (English Edition).

Gao, L.Z., Zhang, C.H., Chen, S.M., Liu, P.J., Ding, X.Z., Liu, Y.X., Dong, C.Y., Song, B., 2010. Detrital zircon SHRIMP U–Pb age from the Diaoyutai Formation, Xihe Group in Liaodong Peninsula, China and its geological significance. Geol. Bull. China 29, 1113–1122 (in Chinese with English abstract).

Goldberg, A.S., 2010. Dyke swarms as indicators of major extensional events in the 1.9–1.2 Ga Columbia supercontinent. J. Geodyn. 50, 176–190.

Griffiths, R.W., Campbell, I.H., 1991. Interaction of mantle plume heads with the Earth's surface and onset of small-scale convection. J. Geophys. Res. 96 (B11), 18295–18310.

GSILP (Geological Survey Institute of Liaoning Province), 2001. Geological Map and Explanation of Changxingdao (J51C001001), Jinzhou (J51C001002), Lüshun (J51C002001) and Dalianshi (J51C002002). Scale 1:250000 (in Chinese).
Halls, H.C., 1982. The importance and potential of mafic dyke swarms in studies of geodynamic process. Geosci. Can. 9, 145–154.
Hanski, E., Mertanen, S., Rämö, T., Vuollo, J. (Eds.), 2006. Dyke Swarms – Time Markers of Crustal Evolution. Taylor & Francis Group, London, 282 p.
Harris, L.B., Li, Z.X., 1995. Palaeomagnetic dating and tectonic significance of dolerite intrusions in the Albany Mobile Belt, Western Australia. Earth Planet. Sci. Lett. 131, 143–164.
He, B., Xu, Y.-G., Chung, S.-L., Xiao, L., Wang, Y., 2003. Sedimentary evidence for a rapid crustal doming before the eruption of the Emeishan flood basalts. Earth Planet. Sci. Lett. 213, 391–405.
Heaman, L., LeCheminant, A.N., 1993. Paragenesis and U–Pb systematics of baddeleyite (ZrO_2). Chem. Geol. 119, 95–126.
Heaman, L.M., 2009. The application of U–Pb geochronology to mafic, ultramafic and alkaline rocks: an evaluation of three mineral standards. Chem. Geol. 261, 43–52.
Hofmann, H.J., Aitken, J.D., 1979. Precambrian biota from the Little Dal Group, Mackenzie Mountains, northwestern Canada. Can. J. Earth Sci. 16, 150–166.
Hoffman, P.F., 1991. Did the breakout of Laurentia turn Gondwanaland inside-out? Science 252, 1409–1412.
Holm, P.M., Heaman, L.M., Pedersen, L.E., 2006. Baddeleyite and zircon U–Pb ages from the Kaerven area, Kangerlussuaq: implications for timing of Paleogene continental breakup in the North Atlantic. Lithos 92, 238–250.
Hong, Z., Huang, Z., Yang, X., Lan, J., Xian, B., Yang, Y., Liu, X., 1988. Medusoid fossils from the Sinian Xingmingcun Formation of southern Liaoning. Acta Geol. Sin. 64, 200–209 (in Chinese with English abstract).
Hou, G., Santosh, M., Qian, X., Lister, G.S., Li, J., 2008. Tectonic constraints on 1.3–1.2 Ga final breakup of Columbia supercontinent from a giant radiating dyke swarm. Gondwana Res. 14, 561–566.
Hu, Z.C., Gao, S., Liu, Y.S., Hu, S.H., Chen, H.H., Yuan, H.L., 2008. Signal enhancement in laser ablation ICP-MS by addition of nitrogen in the central channel gas. J. Anal. At. Spectrom. 23, 1093–1101.
Hu, B., Zhai, M., Li, T., Li, Z., Peng, P., Guo, J., Kusky, T.M., 2012. Mesoproterozoic magmatic events in the eastern North China Craton and their tectonic implications: geochronological evidence from detrital zircons in the Shandong Peninsula and North Korea. Gondwana Res. 22, 828–842.
Irvine, T.N., Baragar, W.R.A., 1971. A guide to the chemical classification of common volcanic rocks. Can. J. Earth Sci. 8, 523–548.
Kamo, S.L., Gower, C.F., Krogh, T.E., 1989. Birthdate for the Iapetus Ocean? A precise U–Pb zircon and baddeleyite age for the Long Range dikes, southeast Labrador. Geology 17, 602–605.
Karlstrom, K.E., Ahall, K.I., Harlan, S.S., Williams, M.L., McLelland, J., Geissman, J.W., 2001. Long-lived (1.8–1.0 Ga) convergent orogen in southern Laurentia, its extensions to Australia and Baltica, and implications for refining Rodinia. Precambrian Res. 111, 5–30.
Kusky, T., Li, J., Santosh, M., 2007. The Paleoproterozoic North Hebei Orogen: North China craton's collisional suture with the Columbia supercontinent. Gondwana Res. 12, 4–28.
Kusky, T.M., Santosh, M., 2009. The Columbia connection in North China. In: Reddy, S.M., Mazumder, R., Evans, D.A.D., Collins, A.S. (Eds.), Palaeoproterozoic Supercontinents and Global Evolution. Geological Society, London, pp. 49–71, Special Publications 323.
Le Bas, M.J., Le Maitre, R.W., Streckeisen, A., Zanettin, B., 1986. A chemical classification of volcanic rocks based on the total alkali-silica diagram. J. Petrol. 27, 745–750.
LBGMR (Liaoning Bureau of Geology and Mineral Resources), 1989. Regional Geology of Liaoning Province. Geological Publishing House, Beijing, 858 p (in Chinese with English abstract).
LBGMR, 1997. Multiple Classification and Correlation of the Stratigraphy of China (21): Stratigraphy (Lithostratic) of Liaoning Province. China University of Geosciences Press, Wuhan, 247 p (in Chinese).
Li, X., Chen, F., Li, Q., Guo, J., 2005. Detrital zircon ages and sources of sedimentary rocks in Penglai Formation, eastern Shandong. Acta Geosci. Sin. 26 (suppl.), 123–124 (in Chinese with English abstract).
Li, Z.X., Bogdanova, S.V., Collins, A.S., Davidson, A., De Waele, B., Ernst, R.E., Fitzsimons, I.C.W., Fuck, R.A., Gladkochub, D.P., Jacobs, J., Karlstrom, K.E., Lu, S., Natapov, L.M., Pease, V., Pisarevsky, S.A., Thrane, K., Vernikovsky, V., 2008. Assembly, configuration, and break-up history of Rodinia: a synthesis. Precambrian Res. 160, 179–210.
Li, H.K., Lu, S.N., Li, H.M., Sun, L.X., Xiang, Z.Q., Geng, J.Z., Zhou, H.Y., 2009a. Zircon and baddeleyite U–Pb precision dating of basic rock sills intruding Xiamaling Formation, North China. Geol. Bull. China 28, 1396–1404 (in Chinese with English abstract).
Li, X.H., Liu, Y., Li, Q.L., Guo, C.H., Chamberlain, K.R., 2009b. Precise determination of Phanerozoic zircon Pb/Pb age by multi-collector SIMS without external standardization. Geochem. Geophys. Geosyst. 10, Q04010, http://dx.doi.org/10.1029/2009GC002400.
Li, Q.L., Li, X.H., Liu, Y., Tang, G.Q., Yang, J.H., Zhu, W.G., 2010. Precise U–Pb and Pb–Pb dating of Phanerozoic baddeleyite by SIMS with oxygen flooding technique. J. Anal. At. Spectrom. 25, 1107–1113.
Lin, W., Wang, Q.C., Wang, J., Wang, F., Chu, Y., Chen, K., 2011. Late Mesozoic extensional tectonics of the Liaodong Peninsula massif: response of crust to continental lithosphere destruction of the North China Craton. Sci. China Earth Sci. 54, 843–857.
Liu, Y.X., Kuang, H.W., Meng, X.H., Ge, M., Cai, G.Y., 2005a. The Neoproterozoic stratigraphic correlation framework in the Jilin-Liaoning-Xuzhou-Huaiyang area. J. Stratigr. 29, 387–396 (in Chinese with English abstract).
Liu, J., Davis, G.A., Lin, Z., Wu, F., 2005b. The Liaonan metamorphic core complex, Southeastern Liaoning Province, North China: a likely contributor to Cretaceous rotation of Eastern Liaoning, Korea and contiguous areas. Tectonophysics 407, 65–80.
Liu, Y.Q., Gao, L.Z., Liu, Y.X., Song, B., Wang, Z.X., 2006. Zircon U–Pb dating for the earliest Neoproterozoic mafic magmatism in the southern margin of the North China Block. Chin. Sci. Bull. 51, 2375–2382.
Liu, Y.S., Hu, Z.C., Gao, S., Günther, D., Xu, J., Gao, C.G., Chen, H.H., 2008. In situ analysis of major and trace elements of anhydrous minerals by LA-ICP-MS without applying an internal standard. Chem. Geol. 257, 34–43.
Liu, Y., Gao, S., Hu, Z., Gao, C., Zong, K., Wang, D., 2010a. Continental and oceanic crust recycling-induced melt-peridotite interactions in the Trans-North China Orogen: U–Pb dating, Hf isotopes and trace elements in zircons of mantle xenoliths. J. Petrol. 51, 537–571.
Liu, Y.S., Hu, Z.C., Zong, K.Q., Gao, C.G., Gao, S., Xu, J., Chen, H.H., 2010b. Reappraisement and refinement of zircon U–Pb isotope and trace element analyses by LA-ICP-MS. Chin. Sci. Bull. 55, 1535–1546.
Liu, S., Hu, R., Gao, S., Feng, C., Coulson, I.M., Feng, G., Qi, Y., 2012. U–Pb zircon age, geochemical and Sr-Nd isotopic data as constraints on the petrogenesis and emplacement time of the Precambrian mafic dyke swarms in the North China Craton (NCC). Lithos 140–141, 38–52.
Liu, S., Hu, R., Gao, S., Feng, C., Coulson, I.M., Feng, G., Qi, Y., Yang, Y., Yang, C., Tang, L., 2013. Zircon U–Pb age and Sr–Nd–Hf isotopic constraints on the age and origin of Triassic mafic dikes, Dalian area, Northeast China. Int. Geol. Rev. 55, 249–262.
Lu, S.N., Zhao, G.C., Wang, H.C., Hao, G.J., 2008. Precambrian metamorphic basement and sedimentary cover of the North China Craton: a review. Precambrian Res. 160, 77–93.
Lu, S.N., Li, H.K., Xiang, Z.Q., 2010. Advances in the study of Mesoproterozoic geochronology in China: a review. Geol. China 37, 1002–1013 (in Chinese with English abstract).
Lu, S.N., Xiang, Z.Q., Li, H.K., Wang, H.C., Chu, H., 2012. Response of the North China Craton to Rodinia supercontinental events – GOSEN joining hypothesis. Acta Geol. Sin. 86, 1376–1406 (in Chinese with English abstract).
Ludwig, K.R., 2003. User's Manual for Isoplot 3.00. A Geochronological Toolkit for Microsoft Excel. Berkeley Geochronology Center, Special Publication No. 4a, Berkeley, California, 70 p.
Luo, Y., Sun, M., Zhao, G.C., Li, S.Z., Xia, X.P., 2006. LA-ICP-MS U–Pb zircon geochronology of the Yushulazi Group in the Eastern Block, North China Craton. Int. Geol. Rev. 48, 828–840.
Mazumder, R., Foulger, G.R., 2004. Large igneous provinces, mantle plumes and uplift: a sedimentological perspective. EOS Trans. 85, American Geophysical Union, Fall Meeting 2004, abstract #V51B-0533.
Meng, X.H., Ge, M., 2002. Research on cyclic sequence, events and formational evolution of the Sino-Korea Plate. Earth Sci. Front. 9 (3), 31–46 (in Chinese with English abstract).
Meyer, R., van Wijk, J., Gernigon, L., 2007. The North Atlantic Igneous Province: a review of models for its formation. In: Foulger, G.R., Jurdy, D.M. (Eds.), Plates, Plumes, and Planetary Processes. Geological Society of America Special Paper 430, pp. 525–552.
Niu, S.W., Zhu, S.X., 2002. On the Huainan Biota. J. Stratigr. 26, 1–8 (in Chinese with English abstract).
Nyblade, A.A., Sleep, N.H., 2003. Long lasting epeirogenic uplift from mantle plumes and the origin of the Southern African Plateau. Geochem. Geophys. Geosyst. 4 (12), 1105, http://dx.doi.org/10.1029/2003GC000573.
Pan, G.Q., Kong, Q.Y., Wu, J.Q., Liu, J.R., Zhang, Q.L., Zhen, J.H., Liu, D.Z., 2000a. Geochemical features of Neoproterozoic diabase sills in Xuzhou-Suzhou area. Geol. J. China Univ. 6, 53–63 (in Chinese with English abstract).
Pan, G.Q., Liu, J.R., Kong, Q.Y., Wu, Q.Q., Zhang, Q.L., Zeng, J.-H., Liu, D.Z., 2000b. Study on Sinian geologic events in Xuzhou-Suzhou Area and discussion on their origin. Geol. J. China Univ. 6, 566–575 (in Chinese with English abstract).
Pearce, J.A., Cann, J.R., 1973. Tectonic setting of basaltic volcanic rocks determined using trace element analysis. Earth Planet. Sci. Lett. 19, 290–300.
Pearce, J.A., Norry, M.J., 1979. Petrogenetic implications of Ti, Zr, Y and Nb variations in volcanic rocks. Contrib. Mineral. Petrol. 69, 33–47.
Peng, P., 2010. Reconstruction and interpretation of giant mafic dyke swarms: a case study of 1.78 Ga magmatism in the North China craton. In: Kusky, T., Zhai, M.-G., Xiao, W.-J. (Eds.), The Evolving Continents: Understanding Processes of Continental Growth. Geological Society, London, pp. 163–178, Special Publications 338.
Peng, P., Bleeker, W., Ernst, R.E., Söderlund, U., McNicoll, V., 2011a. U–Pb baddeleyite ages, distribution and geochemistry of 925 Ma mafic dykes and 900 Ma sills in the North China craton: Evidence for a Neoproterozoic mantle plume. Lithos 127, 210–221.
Peng, P., Zhai, M., Li, Q., Wu, F., Hou, Q., Li, Z., Li, T., Zhang, Y., 2011b. Neoproterozoic (~900 Ma) Sariwon sills in North Korea: Geochronology, geochemistry and implications for the evolution of the south-eastern margin of the North China Craton. Gondwana Res. 20, 243–254.
Peng, T.P., Wilde, S.A., Fan, W.M., Peng, B.X., Mao, Y.S., 2013. Mesoproterozoic high Fe–Ti mafic magmatismin western Shandong, North China Craton: petrogenesis and implications for the final breakup of the Columbia supercontinent. Precambrian Res. 235, 190–207.
Peng, P., 2015. Precambrian mafic dyke swarms in the North China Craton and their geological implications. Sci. China Earth Sci. 58, 649–675.

Péron-Pinvidic, G., Manatschal, G., 2009. The final rifting and evolution at deep magma-poor margins from Iberia-Newfoundland: a new point of view. Int. J. Earth Sci. 98, 1581–1597.
Pesonen, L.J., Elming, S.-A., Mertanen, S., Pisarevsky, S., D'Agrella-Filho, M.S., Meert, J.G., Schmidt, P.W., Abrahamsen, N., Bylund, G., 2003. Palaeomagnetic configuration of continents during the Proterozoic. Tectonophysics 375, 289–324.
Qiao, X., Gao, L., 2000. Earthquake events in Neoproterozoic and Early Paleozoic and its relationship with supercontinental Rodinia in North China. Chin. Sci. Bull. 45, 931–935.
Qiao, X.F., 2002. Intraplate seismic belt and basin framework of Sino-Korean plate in Proterozoic. Earth Sci. Front. 9, 141–149 (in Chinese with English abstract).
Rainbird, R.H., 1993. The sedimentary record of mantle plume uplift preceding eruption of the Neoproterozoic Natkusiak flood basalt. J. Geol. 101, 305–318.
Rainbird, R.H., Ernst, R.E., 2001. The sedimentary record of mantle-plume uplift. In: Ernst, R.E., Buchan, K.L. (Eds.), Mantle Plumes: Their Identification Through Time. Geological Society of America Special Paper 352, Boulder, Colorado, pp. 227–245.
Rogers, J.J.W., Santosh, M., 2002. Configuration of Columbia, a Mesoproterozoic supercontinent. Gondwana Res. 5, 5–22.
Santosh, M., 2010. Assembling North China Craton within the Columbia supercontinent: the role of double-sided subduction. Precambrian Res. 178, 149–167.
Saunders, A.D., Jones, S.M., Morgan, L.A., Pierce, K.L., Widdowson, M., Xu, Y.G., 2007. Regional uplift associated with continental large igneous provinces: the roles of mantle plumes and the lithosphere. Chem. Geol. 241, 282–318.
Sengör, A.M.C., 2001. Elevation as indicator of mantle-plume activity. In: Ernst, R.E., Buchan, K.L. (Eds.), Mantle Plumes: Their Identification Through Time. Geological Society of America Special Paper 352, Boulder, Colorado, pp. 183–225.
Söderlund, U., Ibanez-Mejia, M., El Bahat, A., Ernst, R.E., Ikenne, M., Soulaimani, A., Youbi, N., Cousens, B., El Janati, M., Hafid, A., 2013. Reply to Comment on "U–Pb baddeleyite ages and geochemistry of dolerite dykes in the Bas-Drâa Inlier of the Anti-Atlas of Morocco: newly identified 1380 Ma event in the West African Craton" by André Michard and Dominique Gasquet. Lithos 174, 101–108.
Stephen, M.J., Nicky, W., Bryan, L., 2001. Cenozoic and Cretaceous transient uplift in the Porcupine Basin and its relationship to a mantle plume. In: Shannon, R.M., Haughton, R.D.W., Corcoran, D.V. (Eds.), The Petroleum Exploration of Ireland's Offshore Basins. Geological Society, London, pp. 345–360, Special Publications 188.
Su, W., Li, H., Xu, L., Jia, S., Geng, J., Zhou, H., Wang, Z., Pu, H., 2012. Luoyu and Ruyang Group at the south margin of the North China Craton (NCC) should belong in the Mesoproterozoic Changchengian System: Direct constraints from the LA-ICP-MS U–Pb age of the tuffite in the Luoyukou Formation, Ruzhou, Henan, China. Geol. Surv. Res. 35, 96–108 (in Chinese with English abstract).
Sun, W., Wang, G., Zhou, B., 1986. Macroscopic worm-like body fossils from the Upper Precambrian (900–700 Ma), Huainan district, Anhui, China and their stratigraphic and evolutionary significance. Precambrian Res. 31, 377–403.
Sun, S.S., McDonough, W.F., 1989. Chemical and isotopic systematics of oceanic basalts: implications for mantle composition and processes. In: Sauders, A.D., Norry, M.J. (Eds.), Magmatism in the Ocean Basins. Geological Society, pp. 313–345, Special Publication 42.
Tack, L., Wingate, M.T.D., Liégeois, J.-P., Fernandez-Alonso, M., Deblond, A., 2001. Early Neoproterozoic magmatism (1000–910 Ma) of the Zadinian and Mayumbian Groups (Bas-Congo): onset of Rodinia rifting at the western edge of the Congo craton. Precambrian Res. 110, 277–306.
Taylor, S.R., McLennan, S.M., 1985. The Continental Crust: Its Composition and Evolution. Blackwell Science Publication, Oxford, 312 p.
Tang, Q., Pang, K., Xiao, S., Yuan, X., Ou, Z., Wan, B., 2013. Organic-walled microfossils from the early Neoproterozoic Liulaobei Formation in the Huainan region of North China and their biostratigraphic significance. Precambrian Res. 236, 157–181.
Tang, Q., Pang, K., Yuan, X., Wan, B., Xiao, S., 2015. Organic-walled microfossils from the Tonian Gouhou Formation, Huaibei region, North China Craton, and their biostratigraphic implications. Precambrian Res. 266, 296–318.
Trubitsyn, V.P., Trubitsyn, A.P., 2005. Evolution of mantle plumes and uplift of continents during the Pangea breakup. Russ. J. Earth Sci. 7, ES3001, http://dx.doi.org/10.2205/2005ES000179.
Wang, Z., Tang, Z., Yang, Z., Yang, X., 2000. Ductile tectonic deformation of Mesozoic time in the Dalian area. Seismol. Geol. 22, 379–386 (in Chinese with English abstract).
Wang, Q.H., Yang, D.B., Xu, W.L., 2012. Neoproterozoic basic magmatism in the southeast margin of North China Craton: evidence from whole-rock geochemistry, U–Pb and Hf isotopic study of zircons from diabase swarms in the Xuzhou-Huaibei area of China. Sci. China Earth Sci. 55, 1461–1479.
Wang, Q.H., Yang, H., Yang, D.B., Xu, W.L., 2014a. Mid-Mesoproterozoic (~1.32 Ga) diabase swarms from the western Liaoning region in the northern margin of the North China Craton: Baddeleyite Pb–Pb geochronology, geochemistry and implications for the final breakup of the Columbia supercontinent. Precambrian Res. 254, 114–128.
Wang, Z.J., Huang, Z.G., Yao, J.X., Ma, X.L., 2014b. Characteristics and main progress of "The Stratigraphic Chart of China and Directions". Acta Geosci. Sin. 35, 271–276 (in Chinese with English abstract).
Wang, W., Liu, S.W., Santosh, M., Zhang, L.F., Bai, X., Zhao, Y., Zhang, S.H., Guo, R.R., 2015. 1.23 Ga mafic dykes in the North China Craton reconstruct the Columbia supercontinent. Gondwana Res. 27, 1407–1418.
Wiedenbeck, M., Alle, P., Corfu, F., Griffin, W.L., Meier, M., Oberli, F., Quadt, A.V., Roddick, J.C., Spiegel, W., 1995. Three natural zircon standards for U-Th-Pb, Lu-Hf, trace element and REE analyses. Geostand. Geoanal. Res. 19, 1–23.
Wilde, S.A., Zhao, G.C., Sun, M., 2002. Development of the North China Craton during the Late Archaean and its final amalgamation at 1.8 Ga; some speculations on its position within a global Palaeoproterozoic supercontinent. Gondwana Res. 5, 85–94.
Williams, G.E., Gostin, V.A., 2000. Mantle plume uplift in the sedimentary record: origin of kilometre-deep canyons within late Neoproterozoic successions, South Australia. J. Geol. Soc. Lond. 157, 759–768.
Winchester, J.A., Floyd, P.A., 1977. Geochemical discrimination of different magma series and their differentiation products. Chem. Geol. 20, 325–343.
Wu, F.Y., Yang, J.H., Liu, X.M., 2005. Geochronological framework of the Mesozoic granitic magmatism in the Liaodong Peninsula, Northeast China. Geol. J. China Univ. 11, 305–317 (in Chinese with English abstract).
Xiao, S., Shen, B., Tang, Q., Kaufman, A.J., Yuan, X., Li, J., Qian, M., 2014. Biostratigraphic and chemostratigraphic constraints on the age of early Neoproterozoic carbonate successions in North China. Precambrian Res. 246, 208–225.
Xing, Y., 1989. The Upper Precambrian of China, vol. 3 of "The Stratigraphy of China". Geological Publishing House, Beijing, 314 p (in Chinese).
Xing, Y., Gao, Z., Wang, Z., Gao, L., Yin, C., 1996. Chinese Stratigraphy Catalog: Neoproterozoic. Geological Publishing House, Beijing, 117 p (in Chinese).
Xu, J., Zhu, G., Tong, W.X., Cui, K.R., Lin, Q., 1987. Formation and evolution of the Tancheng–Lujiang wrench fault system: a major shear system to the northwest of the Pacific Ocean. Tectonophysics 134, 273–310.
Xu, Z., Li, D., Li, H., Wang, Z., 1991. Crustal contraction and extension in southern Liaoning. Geol. Rev. 37, 193–202 (in Chinese with English abstract).
Xu, H., Yang, Z., Peng, P., Meert, J.G., Zhu, R., 2014. Paleo-position of the North China craton within the supercontinent Columbia: constraints from new paleomagnetic results. Precambrian Res. 255, 276–293.
Yale, L.B., Carpenter, S.J., 1998. Large igneous provinces and giant dike swarms: proxies for supercontinent cyclicity and mantle convection. Earth Planet. Sci. Lett. 163, 109–122.
Yang, Z., Gang, J., Han, X., Meng, Q., 1996. The metamorphic core-complex structure in south Liaoning. Liaoning Geol. 13, 241–250 (in Chinese with English abstract).
Yang, T.N., Peng, Y., Wang, Z.X., Li, D.Z., Yang, Z.Z., Wang, G.Z., 2002. Nearly N–S compressional deformation of sedimentary cover in the Lushun–Dalian area: intraplate deformation effect of overlying plate on continental deep subduction of the Sulu area. Geol. Bull. China 21, 308–314 (in Chinese with English abstract).
Yang, J.H., Wu, F.Y., Zhang, Y.B., Zhang, Q., Wilde, S.A., 2004. Identification of Mesoproterozoic zircons in a Triassic dolerite from the Liaodong Peninsula, East China. Chin. Sci. Bull. 49, 1958–1962.
Yang, J.H., Wu, F.Y., Chung, S.L., Lo, C.H., Wilde, S.A., Davis, G.A., 2007a. Rapid exhumation and cooling of the Liaonan metamorphic core complex: inferences from $^{40}Ar/^{39}Ar$ thermochronology and implications for Late Mesozoic extension in the eastern North China Craton. Geol. Soc. Am. Bull. 119, 1405–1414.
Yang, J.H., Sun, J.F., Chen, F.K., Wilde, S.A., Wu, F.Y., 2007b. Sources and petrogenesis of Late Triassic dolerite dikes in the Liaodong Peninsula: implications for post-collisional lithosphere thinning of the eastern North China Craton. J. Petrol. 48, 1973–1997.
Yang, T.N., Peng, Y., Leech, M.L., Lin, H.Y., 2011. Fold patterns indicating Triassic constrictional deformation on the Liaodong peninsula, eastern China, and tectonic implications. J. Asian Earth Sci. 40, 72–83.
Yang, D.B., Xu, W.L., Xu, Y.G., Wang, Q.H., Pei, F.P., Wang, F., 2012. U–Pb ages and Hf isotope data from detrital zircons in the Neoproterozoic sandstones of northern Jiangsu and southern Liaoning Provinces, China: implications for the Late Precambrian evolution of the southeastern North China Craton. Precambrian Res. 216–219, 162–176.
Yin, L., 1991. Late Proterozoic microfossils from the Tongjiazhuang Formation, western Shandong, China. Acta Micropalaeontol. Sin. 8, 253–269 (in Chinese with English abstract).
Yin, L., Sun, W., 1994. Microbiota from the Neoproterozoic Liulaobei Formation in the Huainan region, northern Anhui, China. Precambrian Res. 65, 95–114.
Zang, W., Walter, M.R., 1992. Late Proterozoic and Early Cambrian microfossils and biostratigraphy, northern Anhui and Jiangsu, central-eastern China. Precambrian Res. 57, 243–323.
Zhai, M., Shao, J., Hao, J., Peng, P., 2003. Geological signature and possible position of the North China Block in the supercontinent Rodinia. Gondwana Res. 6, 171–183.
Zhai, M.G., 2004. Precambrian tectonic evolution of the North China Craton. In: Malpas, J., Fletcher, C.J.N., Ali, J.R., Aitchison, J.C. (Eds.), Aspects of the Tectonic Evolution of China. Geological Society, pp. 57–72, Special Publications 226.
Zhai, M.G., Santosh, M., 2013. Metallogeny of the North China Craton: link with secular changes in the evolving Earth. Gondwana Res. 24, 275–297.
Zhang, S., Li, Z.X., Wu, H., 2006. New Precambrian palaeomagnetic constraints on the position of the North China Block in Rodinia. Precambrian Res. 144, 213–238.
Zhang, S.H., Zhao, Y., Yang, Z.Y., He, Z.F., Wu, H., 2009. The 1.35 Ga diabase sills from the northern North China Craton: implications for breakup of the Columbia (Nuna) supercontinent. Earth Planet. Sci. Lett. 288, 588–600.
Zhang, S.H., Zhao, Y., Santosh, M., 2012a. Mid-Mesoproterozoic bimodal magmatic rocks in the northern North China Craton: implications for magmatism related to breakup of the Columbia supercontinent. Precambrian Res. 222–223, 339–367.
Zhang, S., Li, Z.X., Evans, D.A.D., Wu, H., Li, H., Dong, J., 2012b. Pre-Rodinia supercontinent Nuna shaping up: a global synthesis with new paleomagnetic results from North China. Earth Planet. Sci. Lett. 353–354, 145–155.
Zhao, G.C., Cawood, P.A., Wilde, S.A., Sun, M., 2002. A review of the global 2.1–1.8 Ga orogens: implications for a pre-Rodinian supercontinent. Earth Sci. Rev. 59, 125–162.

Zhao, G.C., Sun, M., Wilde, S.A., Li, S.Z., 2003. Assembly, accretion and breakup of the Paleo-Mesoproterozoic Columbia Supercontinent: records in the North China Craton. Gondwana Res. 6, 417–434.
Zhao, G.C., Sun, M., Wilde, S.A., Li, S., 2004. A Paleo-Mesoproterozoic supercontinent: assembly, growth and breakup. Earth Sci. Rev. 67, 91–123.
Zhao, G.C., Sun, M., Wilde, S.A., Li, S.Z., Zhang, J., 2006. Some key issues in reconstructions of Proterozoic supercontinents. J. Asian Earth Sci. 28, 3–19.
Zhao, G.C., Li, S.Z., Sun, M., Wilde, S.A., 2011. Assembly, accretion, and break-up of the Palaeo-Mesoproterozoic Columbia supercontinent: record in the North China Craton revisited. Int. Geol. Rev. 53, 1331–1356.
Zhao, G.C., Zhai, M.G., 2013. Lithotectonic elements of Precambrian basement in the North China Craton: review and tectonic implications. Gondwana Res. 23, 1207–1240.
Zhao, G.C., 2014. Precambrian Evolution of the North China Craton. Elsevier, Amsterdam, 194 p.
Zheng, W., 1979. Principal characteristics of “Huainan biota” and its stratigraphic significance. J. Hefei Polytech. Univ. 2, 97–108 (in Chinese with English abstract).
Zhu, G., Wang, Y.S., Liu, G.S., Niu, M.L., Xie, C.L., Li, C.C., 2005. $^{40}Ar/^{39}Ar$ dating of strike-slip motion on the Tan-Lu fault zone, East China. J. Struct. Geol. 27, 1379–1398.